

DEVELOPMENT OF MULTIPLE SAMPLE SOLID-STATE NMR PROBES FOR ANALYSIS  
OF PHARMACEUTICAL COMPOUNDS AND FORMULATIONS

BY

Copyright 2011

Benjamin N. Nelson

Submitted to the graduate degree program in Pharmaceutical Chemistry and the Graduate  
Faculty of the University of Kansas in partial fulfillment of the requirements for the degree of  
Doctor of Philosophy.

---

Chairperson Jennifer S. Laurence

---

Eric J. Munson

---

John F. Stobaugh

---

Cory Berkland

---

Susan M. Lunte

---

Robert G. Carlson

Date Defended: June 1, 2011

The Dissertation Committee for Benjamin N. Nelson

certifies that this is the approved version of the following dissertation:

DEVELOPMENT OF MULTIPLE SAMPLE SOLID-STATE NMR PROBES FOR ANALYSIS  
OF PHARMACEUTICAL COMPOUNDS AND FORMULATIONS

---

Chairperson Jennifer S. Laurence

Date approved: June 1, 2011

## **Abstract**

Solid-state NMR spectroscopy (ssNMR) is an extremely powerful technique for the analysis of pharmaceutical dosage forms. A major limitation of ssNMR is the number of samples that can be analyzed in a given period of time. Development of three versions of probes that contain multiple magic angle spinning (MAS) modules for interleaved acquisition has been done, and each shows no loss in spectral quality compared to a standard probe. A prototype probe incorporating two MAS modules was first developed. This version is limited to being a two-module probe due to the large amounts of space required for the tuning elements, which are located next to the MAS modules. A new probe design incorporating coaxial transmission lines and smaller MAS modules has also been constructed. This probe allows for close proximity of the MAS modules (within 3 cm) and the capability of remote tuning and sample changing. This probe design can be easily scaled to incorporate more than two MAS modules, which is a limitation of the previous design. The number of modules that can be incorporated is only limited by the number of transmission lines that will fit in a cross-sectional diameter of the bore and the axial field length of the magnet. A third version addresses the main issues of length and linear actuation that the first generation probes have. So that the superconducting magnet can be left at “factory” height, a non-actuated probe that has the ability to collect two samples at a time has been constructed and tested. The radio frequency circuits have been isolated to such a degree that they do not dramatically affect the spectra of one another. Spectra of ssNMR standards: methylglutaric acid, hexamethylbenzene, and adamantane were acquired to show comparable performance of all multiple sample probe versions and conventional probes.

## **Acknowledgements**

There are several people I would like to thank for supporting me during my academic journey. During my final year at St. Norbert College (SNC), I went on a geology trip to Costa Rica, where my post-secondary academic journey began. One night in a cantina in Monte Verde Dr. Tim Flood said “Ben, it is obvious you are not stupid. You need to go to graduate school.” Upon our return I checked in with my advisor Dr. David Klopotek. Dr. Klopotek agreed with Dr. Flood’s assessment and arranged a fateful meeting with, Dr. Joe Vitt, Professor of Chemistry at The University of South Dakota (USD) that same week. Dr. Vitt was visiting SNC as a guest lecturer. Dr. Vitt informed me that several SNC professors had assured him that my intellect was not accurately reflected in my official academic record. He trusted their opinion and suggested that I continue my academic career at USD, where they would “straighten” me out. Upon my arrival, Dr. Mary Berry encouraged me to join her lab group. With Dr. Berry’s help I received the “Most Outstanding Graduate Student Award,” upon my graduation, with honors as a Master in Physical Chemistry. I had been successfully straightened out, at least academically.

While at USD, I had the opportunity to meet with another guest lecturer, Dr. Eric Munson, Professor of Pharmaceutical Chemistry at the University of Kansas (KU). Dr. Munson assured me that a physical chemist would excel in the pharmaceutical chemistry department at KU, the birthplace of physical pharmacy. I joined the Munson lab group where I was introduced to NMR, and was able to combine my love of learning with my love of designing and building things. I will always be thankful for the experience and knowledge I gained from Dr. Munson and fellow members of his lab group. My

experience at KU, was enriched with the addition of Dr. Jennifer Laurence, as Chair of my thesis committee. Dr. Laurence graciously volunteered to replace Dr. Munson as Chair of my thesis committee, after his departure from KU. Her help in the final stretch of my journey has been immeasurable. Her willingness, encouragement and enthusiasm in working with me, further demonstrates that she deserved to be recognized as a recipient of the Louise Byrd Graduate Educator Award.

In addition to professors, I have also been fortunate to work with several individuals who work outside of the Pharmaceutical Chemistry department at KU. My experience at KU would not be complete without their assistance and insight. A special thanks goes out to Charles Gabel and Ash Shadrack at the Mechanical Engineering Machine Shop at KU. Charles and Ash allowed me to work in their shop and create part after part for the probes I designed. Without the use of their shop and expertise I could not have built all of my probes. Without their friendship, there were times I may have lost my mind. After a chance encounter at the bowling alley, I met Ben Panzer, who shares many recreational interests with me. Ben is also an electrical engineering student at KU. Ben, who is an expert with RF circuits, has helped me with the accuracy of the RF sections of this dissertation (without excessive chastisement for using NMR “lingo” when talking about RF). I would also like to thank him for the motivational phrase “Team Ben for the win” and his friendship.

Personally, I would like to thank Brett and Casey Toomay. My family is grateful to have friends like them, always there to listen or help take your mind off troubles. We joke that we have parallel lives, sharing many of the same life experiences. We have even been able to discover and share the joys of parenthood with them. Their daughter,

Ryan and our son, Finn were born within a few weeks of each other and are best friends. They have recently informed us that they are girlfriend and boyfriend.

Lastly, I would like to extend a heart-felt thanks to my family. My parents Lyle and Monica, along with my brother Greg, have always been supportive of my perpetual education. They were instrumental in showing me the rewards of learning, by continually placing new challenges in front of me. I am also thankful for the support of my in-laws, Tom and Mary Sue Leland, who have been so supportive of my education; even after I have slowly moved their daughter further and further from Wisconsin. And last, but not least, I thank my wife Heidi and our children, Finn and Liesl. Although their lives have been impacted daily, they continue to love me unconditionally. They are the best family I could ever ask for; they have put up with a lot from me and I love them very much.

## Table of Contents

<b>Abstract.....</b>	<b>iii</b>
<b>Table of Contents .....</b>	<b>vii</b>
<b>List of Tables .....</b>	<b>viii</b>
<b>List of Figures.....</b>	<b>ix</b>
<b>Partial List of Abbreviations.....</b>	<b>x</b>
<b>Chapter 1 Introduction.....</b>	<b>1</b>
1.1 Purpose.....	2
1.2 The Solid-state NMR Experiment .....	2
1.3 Transmission Line RF Circuits.....	5
<b>Chapter 2 Multiple-Sample Solid-State NMR Probe with Lumped-Element Tuning.....</b>	<b>16</b>
2.1 Introduction.....	17
2.2 Experimental .....	19
2.2.1 Probe concept .....	19
2.2.2 Effect of Magnetic Field Strength along Superconducting Solenoid Axis.....	23
2.2.3 Solid-State NMR Spectra .....	27
2.3 Results .....	27
2.4 Conclusion .....	32
2.5 References.....	32
<b>Chapter 3 Multiple-Sample Solid-State NMR Probe with Three-Quarter Wavelength Coaxial Transmission Lines .....</b>	<b>34</b>
3.1 Introduction.....	35
3.2 Experimental .....	39
3.2.1 Probe Construction.....	39
3.2.2 Solid-State NMR Spectra .....	43
3.3 Results .....	43
3.4 Conclusions.....	48
3.5 References.....	49
<b>Chapter 4 Non Moving Multiple-Sample Solid-State NMR Probe .....</b>	<b>50</b>
4.1 Introduction.....	51
4.2 Experimental .....	53
4.2.1 Probe concept .....	53
4.2.2 Probe Construction.....	58
4.2.3 Solid-State NMR Spectra .....	60
4.3 Results .....	61
4.3.1 Homogeneity and Signal to Noise Ratio .....	61
4.3.2 RF Isolation .....	66
4.4 Conclusions.....	72
4.5 References.....	72

## List of Tables

<b>Table 1.1</b>	<b>Recycle delays for various pharmaceutical compounds .....</b>	<b>10</b>
<b>Table 3.1</b>	<b>90° pulse width and SNR of various coils and probes .....</b>	<b>40</b>
<b>Table 4.1</b>	<b>Xylose peak intensities for experiments in coil coupling .....</b>	<b>69</b>



## List of Figures

Figure 1.1 Voltage and current variation along an open circuited transmission line .....	6
Figure 1.2 Tuning circuit for a quarter-wave transmission line NMR probe .....	7
Figure 2.1 Relative magnitudes of $T_2$ and $T_1$ for solution and solid-state NMR.....	18
Figure 2.2 Basic concept for mss probe .....	20
Figure 2.3 Theoretical arrangement for multiple experiments with mss probe .....	21
Figure 2.4 Positions of MAS modules in the bore of a 9.4 Tesla magnet.....	24
Figure 2.5 Picture of mss probe with lumped element tuning .....	25
Figure 2.6 Picture of probe in magnet .....	27
Figure 2.7 HMB spectra for SNR measurements .....	29
Figure 2.8 HMB spectrum with choreographed pulse sequence and movement.....	30
Figure 2.9 Spectra of ibuprofen and aspirin with and without movement.....	32
Figure 3.1 Tuning circuit for a double resonance $3\lambda/4$ transmission line probe.....	37
Figure 3.2 Picture of single module $3\lambda/4$ transmission line probe.....	38
Figure 3.3 Picture of two styles of MAS modules .....	39
Figure 3.4 Principle views of 4-module mss probe engineering assembly .....	41
Figure 3.5 X and H tuning circuits for a single channel of the 4-module mss probe.....	42
Figure 3.6 FID of MGA in all modules of mss probe.....	46
Figure 3.7 Individual spectra of MGA collected simultaneously in mss probe.....	47
Figure 3.8 Spectra of lactose collected with and without probe movement .....	49
Figure 4.1 Principle views of nm-mss probe top section engineering assembly.....	54
Figure 4.2 Principle views of nm-mss probe bottom section engineering assembly .....	55
Figure 4.3 Arrangement of MAS modules in homogeneous regions of the magnet .....	56
Figure 4.4 Block diagrams of $^{13}\text{C}$ receiver sections .....	60
Figure 4.5 $^{13}\text{C}$ spectrum of adamantane from top MAS module of nm-mss probe.....	63
Figure 4.6 $^{13}\text{C}$ spectrum of adamantane from bottom MAS module of nm-mss probe .....	64
Figure 4.7 $^{13}\text{C}$ spectrum of HMB from nm-mss and conventional probes .....	65
Figure 4.8 $^{13}\text{C}$ spectrum of MGA from nm-mss and conventional probes.....	66
Figure 4.9 $^{13}\text{C}$ spectra of MGA acquired using superior $^{13}\text{C}$ receiver section .....	67
Figure 4.10 Noise region of HMB $^{13}\text{C}$ spectrum showing no crosstalk.....	68
Figure 4.11 $^{13}\text{C}$ spectra of xylose with MGA pulses prior to acquisition.....	70
Figure 4.12 Graph of sample coil coupling vs. cable length.....	71
Figure 4.13 Depiction of theoretical deconstructive interference.....	72

### Partial List of Abbreviations

ssNMR	solid-state NMR
MAS	magic angle spinning
RF	radio frequency
B <sub>0</sub>	static magnetic field
CSA	chemical shift anisotropy
TPPM	two pulse phase modulation
SPINAL-64	small phase incremental alteration, with 64 steps
CP	cross polarization
$\gamma$	magnetogyric ratio
T <sub>1</sub>	longitudinal or spin-lattice relaxation constant
T <sub>2</sub>	transverse or spin-spin relaxation constant
$\lambda/4$	quarter-wavelength
$3\lambda/4$	three-quarter-wavelength
SNR	signal to noise ratio
FID	free induction decay
FT	Fourier transform
PD	pulse delay
HMB	hexamethylbenzene
MGA	methylglutaric acid
mss probe	multiple-sample solids probe
nm-mss probe	non-moving multiple-sample solids probe

## **Chapter 1**

### **Introduction**

## 1.1 Purpose

In this dissertation the development of multiple-sample solid-state nuclear magnetic resonance probes will be discussed. These probes have been developed to address the need to increase throughput of the technique. Because of the time it takes to generate quality spectra, solid-state NMR is not used with the frequency of other analytical techniques in the drug development process. With higher throughput capabilities more pharmaceutical compounds can be analyzed yielding vast quantities of information about pharmaceuticals, which will lead to higher quality products for patients, faster and cheaper.

## 1.2 The Solid-state NMR Experiment

It is necessary to understand the differences between NMR of liquids and solids, and the requirements in probe design that these differences cause. With solid-state NMR (ssNMR) there are a number of orientation-dependent effects associated with the crystal lattice that are averaged to zero in solution. Specifically to be discussed are dipolar interaction, chemical shift anisotropy, and cross polarization.

The dipolar field of a NMR active nucleus is aligned with the static magnetic field ( $B_0$ ), in either additive or subtractive fashion. The orientation of an internuclear vector in the presence of a static magnetic field ( $B_0$ ) is described by two angles.  $\theta$  is the angle between the internuclear vector and  $B_0$ , while  $\Phi$  is its rotation about  $B_0$ . The field experienced by a neighbor nucleus is independent of  $\Phi$ , but depends on  $\theta$  by:

$$3\cos^2\theta - 1 \tag{1.1}$$

The magnitude of the dipolar field is twice as strong when  $\theta=0^\circ$  (parallel to  $B_0$ ) than when  $\theta=90^\circ$  (orthogonal to  $B_0$ ). There are an infinite number of orientations of  $\theta=90^\circ$  about the  $B_0$  axis, which leads to many more possible values of  $\Phi$  when  $\theta=90^\circ$ . All possible orientations are averaged in the liquid state, resulting in an overall averaged dipolar field of zero. In solids, all possible internuclear vectors orientations are present, but fixed for each dipolar pair. The result is broad lines in the ssNMR spectrum. In attempt to reduce the effects of dipolar coupling magic angle spinning (MAS) and radio frequency (RF) decoupling are used.

MAS[1] is the rotation of a sample at the magic angle, with respect to  $B_0$ , at frequencies of thousands of Hertz. The magic angle is the angle that causes Eq. 1.1 to go to zero, and is equal to  $\arctan\sqrt{2}$ , or approximately  $54.74^\circ$ . It is also described as the angle of a line from the lower left front corner of a cube to the upper right rear corner. When a sample is rotated at the magic angle the dipolar effects are averaged, and can become zero if the speed is fast enough (greater than 5 times the interaction in Hertz). Another orientation dependent effect, chemical shift anisotropy (CSA), is caused by the asymmetrical circulation of electrons about the nucleus, and can also be averaged via MAS. Heteronuclear couplings between carbon and hydrogen are generally too great to overcome using MAS, so RF decoupling[2] must be used. The basic premise of RF decoupling is that if a field is applied to a nucleus that repeatedly changes its spin state rapidly enough, the neighboring nucleus sees an average effect, thereby reducing the complexity of the spectrum by removing orientation dependent differences. Amplitude modulated decoupling sequences have been developed that perform better than continuous wave decoupling. Two pulse phase modulation (TPPM)[3] and small phase

incremental alteration, with 64 steps (SPINAL-64)[4] are the two modulated sequences used to decouple protons from carbons during  $^{13}\text{C}$  ssNMR data collection of all spectra in this document.

A technique commonly used in ssNMR is cross polarization (CP), which transfers magnetization between heteronuclei. The magnetic moment of a nucleus is proportional to its spin angular momentum with the proportionality constant called the magnetogyric ratio ( $\gamma$ ).  $^{13}\text{C}$  has a  $\gamma$  that is 25% of  $^1\text{H}$ , making its magnetic moment smaller and causing it to be a less sensitive nucleus. CP is used to enhance the magnetization of  $^{13}\text{C}$  by transferring to it the magnetization of neighboring protons, in turn enhancing the signal in the  $^{13}\text{C}$  spectrum.

An added benefit of the CP experiment is a shortened recycle delay. After a transient acquisition, the magnetic moments of the nuclei need to be allowed to relax back to equilibrium, or to re-align with  $B_0$ . The time constant for the process,  $T_1$ , is known as the spin-lattice relaxation time constant or the longitudinal relaxation time constant. For most experiments it is required to have recycle delay 3-5 times  $T_1$ . Protons have much faster longitudinal relaxation rates, and the CP experiment pulse delay depends only on the  $^1\text{H}$   $T_1$  and not the much longer  $^{13}\text{C}$   $T_1$ .

What does this mean to the ssNMR probe designer? Probes must contain MAS spinning modules, which require delivery of compressed air through dedicated lines. Double resonance tuning circuits are required for CP and RF decoupling. These circuits must be robust enough to handle sufficient RF power to produce decoupling fields of greater than 60 kHz, or greater than 5 times the rate of interaction of neighboring dipolar

nuclei. Because of this, designing and engineering ssNMR probes is technically challenging.

### 1.3 Transmission Line RF Circuits

A rigid coaxial transmission line consists of an inner conductor mounted concentrically inside a tubular outer conductor. The two conductors are insulated from each other via small dielectric spacers. The purpose of the transmission line is to transfer the energy output of the transmitter to the antenna with the least possible power loss. For NMR the spectrometer is the transmitter and the sample coil is the antenna.

At a length,  $z$  (defined as positive towards the sample coil), from the sample coil the voltage ( $V(z)$ ) and current ( $I(z)$ ) on an open circuited transmission line are:

$$V(z) = 2V_0^+ \cos \beta z \quad (1.2)$$

$$I(z) = \frac{-2jV_0^+}{Z_0} \sin \beta z \quad (1.3)$$

where  $V_0^+$  is the incident voltage in the positive  $z$  direction,  $Z_0$  is the characteristic impedance,  $j$  is equal to  $-\sqrt{-1}$  (-i), and  $\beta$  is equal to  $\frac{2\pi}{\lambda}$ . Equations 1.2 and 1.3 are plotted in Figure 1.1 with length,  $z$ , as the X-axis, and normalized amplitude[5].

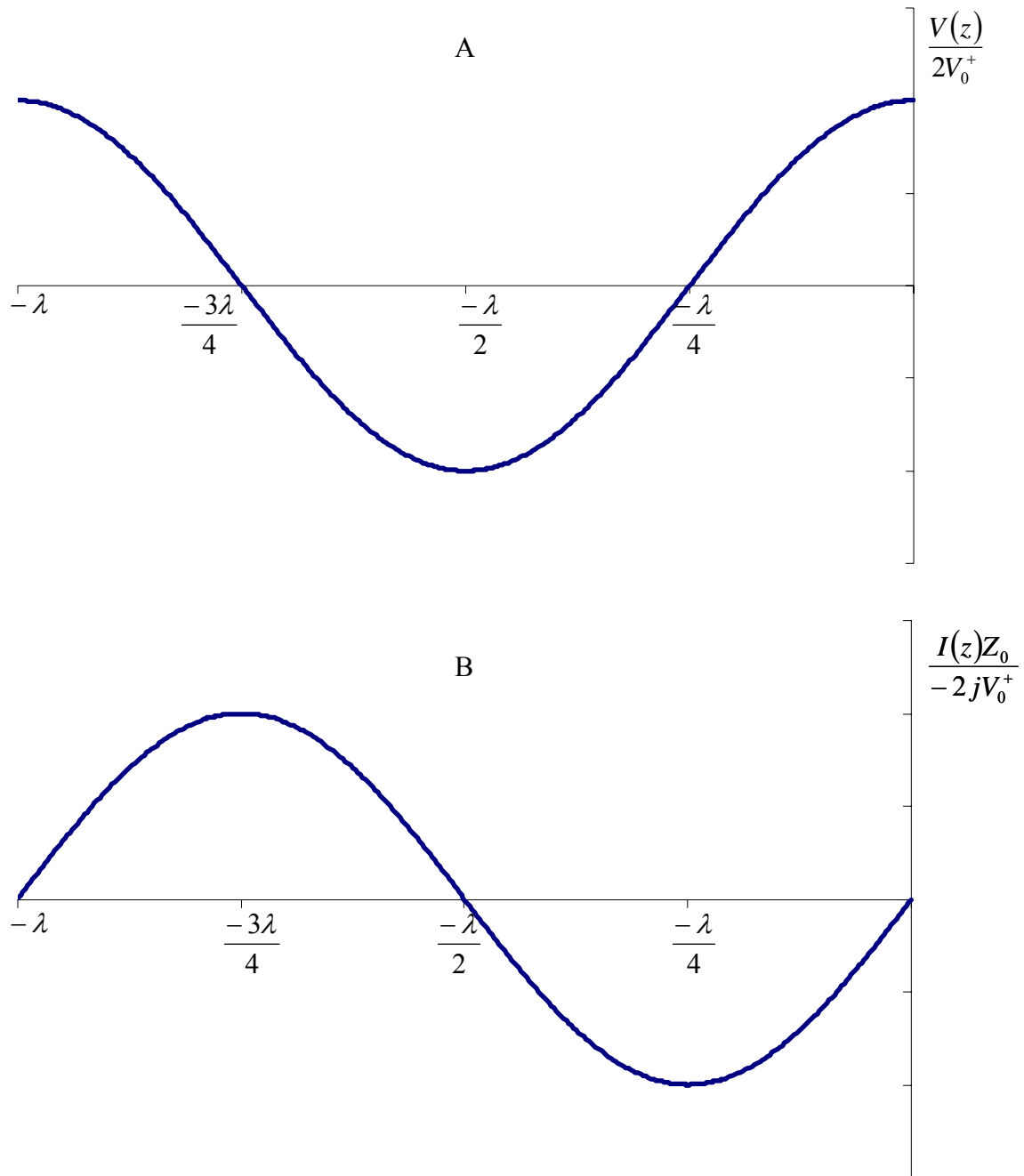


**Figure 1.1 A) Voltage and B) current variation along an open circuited transmission line.**

It is important to note the voltage of the wave equals zero at odd  $\lambda/4$  lengths, as can be seen in Figure 1.1-A. At this zero voltage point, commonly referred to as the tap point, a second RF frequency can be added to the transmission line in order to deliver two RF



frequencies to the sample coil with a single transmission line. For an H-X NMR probe the  $\lambda/4$  of the higher H RF frequency is used and the X RF is tapped in at the voltage null, effectively isolating the inputs of the two circuits.

The transmission line is not exactly a  $\lambda/4$  in length; however, it is extended a short distance. The input impedance looking into the coil is inductive, but when looking at this same input impedance from the input of the transmission line it is capacitive. To make this input impedance seen from the input of the quarter-wave transmission line inductive, and thus cancel the reactance with a series capacitor, an extra length of transmission line was added. The network of parallel variable capacitors, VMC and VTC shown in Figure 1.2, dictates the resonance frequencies of the circuits and cancels the reactance of the coil.

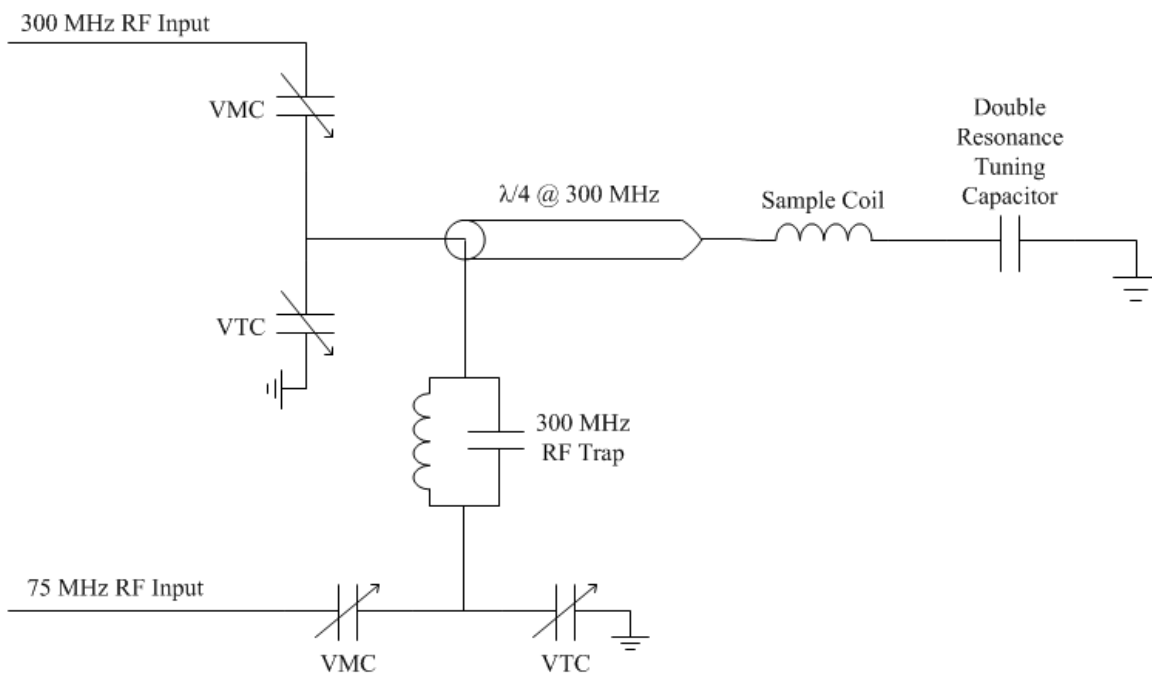


**Figure 1.2. Tuning circuit for a quarter-wave transmission line double resonance NMR probe (VMC and VTC are Variable Match and Tune Capacitors).**

#### 1.4 Solid-state NMR of Pharmaceuticals

Solid-state NMR spectroscopy (ssNMR) is a very powerful technique for the analysis of pharmaceuticals and pharmaceutical formulations, because of the vast quantity of information obtained about the structure and dynamics of compounds in a formulation.[6-8] ssNMR has the capability to determine the state of a drug either in the bulk state or within a formulated product without having to extract the drug from the formulation. It is selective, in that the drug usually has a different chemical shift than that of the excipients, making it easy to identify the drug in the formulation. Since ssNMR is quantitative, it can be used to determine the relative amounts of different crystalline forms and amorphous content. Drug–excipient interactions can also be studied. Determination of mobilities can help identify why a drug may have failed (or will fail) stability tests. Controlled-release devices are complex systems which could be much better formulated if the state of the drug could be determined directly, which is possible using ssNMR.

New drug compounds are often poorly crystalline or even amorphous, have long relaxation times, and are present at low levels in a formulation. This creates a significant problem for analyzing these compounds with ssNMR. Analysis times can range from a few minutes to a few days, depending upon the state of the sample (i.e. bulk drug or formulated product; crystalline or amorphous), relative sensitivity (i.e. choice and number of different nuclei in molecule), and relaxation parameters. For example, quantitation of a mixture of two forms of a compound can take a few hours (for a sample with short relaxation times) to a few days. Analyzing a series of formulated products may take a month or more of spectrometer time. This leads to low throughput, high cost

per sample analysis, and has relegated ssNMR in many cases to be a prohibitively expensive problem-solving technique compared to other analytical techniques such as powder X-ray diffraction (PXRD), infrared and Raman spectroscopy, and differential scanning calorimetry (DSC). Improving throughput of ssNMR would enable better formulation because of the inability to gain such specific information via other techniques.

Increasing the signal to noise ratio (SNR) by signal averaging (in samples containing nuclei with low magnetogyric ratios, low natural abundance, and low sample concentration) is a problem if the sample has long spin-lattice relaxation times ( $T_1$ ) of minutes, hours, or even days, because the number of transients acquired is limited to one to several dozen. Table 1.1 shows the relaxation times for many pharmaceutical solids reported in the literature.[9-15]

**Table 1.1. Recycle delays for various pharmaceutical compounds.**

Compound	<sup>1</sup> H Frequency	Delay (s)	Delay at 9.4 T (s)	Ref
R.O.Y.*	300	40-70	70-125	4
Cimetidine	360	15	18	5
LY297802	400	5-10	5-10	6
Ephedrine	200	1.5	6	7
Aspirin	300	90	160	†
Salicylic Acid	300	1000	1780	†
Prednisolone t-Butylacetate	200	3	12	8
Acetaminophen	200	2	8	9
Carbamazepine	200	3	12	10
Enalapril Maleate	200	2	8	9
Ibuprofen	200	2	8	9
*5-methyl-2-[(2-nitrophenyl)amino]-3-thiophenecarbonitrile, †from our laboratory				

For example, aspirin is a representative pharmaceutical solid that has a <sup>1</sup>H T<sub>1</sub> relaxation time of approximately 30 s at 300 MHz. In a <sup>13</sup>C cross polarization magic-angle spinning (CPMAS) experiment the delay between acquisitions must be greater than 90 s to avoid saturation. Supposing 40 transient acquisitions are required for adequate SNR of a pure aspirin sample, the experimental time would be 1 hour. For a formulation in which aspirin were to only make up a small percentage of the total mass, it may require 2000 transient acquisitions for adequate SNR, which would take over 2 days. Note that some of the compounds listed in Table 1.1, from sources outside our laboratory, may have been chosen for study via ssNMR because they have relatively short relaxation times.

The SNR in an NMR experiment is proportional to the signal divided by the noise.[16] The two most common approaches to improve SNR are to increase signal or

decrease noise (or both). One potential solution to increasing signal is higher magnetic field strengths, but that also has several disadvantages for solid pharmaceuticals. First, resolution often will not increase dramatically at higher fields if the sample line width is limited by bulk magnetic susceptibility or a range of conformations (as in amorphous materials). Second, higher fields require faster spinning speeds to obtain the same separation in parts per million (ppm) between isotropic peaks and spinning sidebands. This implies smaller sample volumes and less signal. Third, for crystalline solids, especially those without methyl groups, the relaxation rate is often inversely proportional to the square of the magnetic field strength.[17, 18] Going from 7.05 T to 18.8 T could potentially increase relaxation delays by about a factor of seven, significantly mitigating any sensitivity gains obtained by going to higher field strengths. Another method to increase signal intensity is to increase the sample volume. However, there are several significant limitations to the development of a large MAS probe capable of CP and high-power  $^1\text{H}$  decoupling. These include producing a high-power  $^1\text{H}$  RF field capable of minimal decoupling for a moderately rigid proton environment, the ability to spin a large sample at the magic angle with minimal sidebands, and producing a homogeneous magnetic field over the entire sample. In fact, the directions of research in MAS has been to decrease sample size. Finally, lowering the temperature of the coil and other electronics can reduce noise, and is the approach taken in the cryoprobe.[19, 20] The sensitivity gains arise from lower noise figures for both the coil and the preamplifier, and a higher Q (quality factor).[19] Some sacrifice is made in filling factor, which limits the gains in sensitivity. In the solid state, especially for MAS systems, cooling the coil without cooling the sample would be extraordinarily difficult, although there are current

research efforts in this area.[21] Even cooling the entire MAS system is technically challenging.

### **1.5 Previous Attempts of Throughput Improvement**

Oldfield recognized almost a decade ago that throughput was a significant issue on high-field NMR spectrometers.[22] He designed a probe that contained three different samples simultaneously located in the homogeneous region of the magnetic field. Although in his design all of the samples were static, he proposed that at least one could incorporate sample spinning. The resolution of this system was quoted as  $\sim 1$  ppm. This concept has been extended to solution NMR spectroscopy.[23-30] Raftery and coworkers have shown that up to four different samples could be located simultaneously in the homogeneous region of the magnetic field.[23] However, the increase in the number of samples simultaneously present in the homogeneous region of the magnetic field comes at a cost of smaller sample volumes. This design does not easily allow for incorporation of MAS for multiple samples at typical ( $0.5 \text{ cm}^3$ ) solid sample sizes. The approach does not provide sufficient improvement to enable practical pharmaceutical analysis. The research presented in this dissertation has expanded the use of ssNMR for such purposes by taking advantage of fundamental and engineering innovations. Chapter 2 describes the design and testing of a proof of concept probe. The design is limited to 2 MAS modules, but shows that the theory of multiple-sample ssNMR probes is relatively sound. Chapter 3 shows how the probe was scaled to include more MAS modules. Drastic redesign of the method for tuning the probe is shown to allow room for 4 MAS modules, and have the adjustable elements of the tuning circuits located outside of the

magnet dewar for easy access. Both probe prototypes in chapters 2 and 3 require actuation of the probe up and down in the bore of the magnet to acquire the spectra of the multiple samples. Chapter 4 proposes a design which has 2 MAS modules and does not require shuttling of the probe in the magnet bore.

## 1.6 References

1. Andrew, E.R., A. Bradbury, and R.G. Eades, *Nuclear Magnetic Resonance Spectra From a Crystal Rotated at High Speed*. Nature, 1958. **182**: p. 1659.
2. Bloch, F., *Theory of Line Narrowing by Double-Frequency Irradiation*. Physical Review, 1958. **111**: p. 841-853.
3. Bennett, A.E., et al., *Heteronuclear decoupling in rotating solids*. Journal of Chemical Physics, 1995. **103**(16): p. 6951-8.
4. Fung, B.M., A.K. Khitrin, and K. Ermolaev, *An Improved Broadband Decoupling Sequence for Liquid Crystals and Solids*. J Magn Reson, 2000. **142**: p. 97-101.
5. Pozar, D.M., *Microwave Engineering*. Third ed. 2005, Hoboken, NJ: John Wiley & Sons, Inc.
6. Bugay, D.E., *Solid-State Nuclear Magnetic Resonance Spectroscopy: Theory and Pharmaceutical Applications*. Pharm. Res., 1993. **10**: p. 317-327.
7. Bugay, D.E., *Magnetic Resonance Spectrometry*, in *Physical Characterization of Pharmaceutical Solids*, H.G. Brittain, Editor. 1995, Marcel Dekker, Inc.: New York. p. 93-125.
8. Offerdahl, T.J. and E.J. Munson, *Solid-State NMR Spectroscopy of Pharmaceutical Materials*. Am. Pharm. Rev., 2004: p. in press.
9. Smith, J., et al., *Application of Two-Dimensional  $^{13}\text{C}$  Solid-State NMR to the Study of Conformational Polymorphism*. J. Am. Chem. Soc., 1998. **120**: p. 11710-11713.

10. Middleton, D.A., et al., *A Cross-Polarization Magic-Angle Spinning  $^{13}\text{C}$  NMR Characterization of the Stable Solid-State Forms of Cimetidine*. J. Pharm. Sci., 1997. **86**: p. 1400-1402.
11. Reutzel, S.M. and V.A. Russell, *Origins of the Unusual Hygroscopicity Observed in LY297802 Tartrate*. J. Pharm. Sci., 1998. **87**: p. 1568.
12. Schmidt, W.F. and I.L. Honigberg, *Nuclear Magnetic Resonance (NMR) Spectroscopic Investigation of Interaction Energies of Ephedrine Stereoisomers in Non Crystalline Solids and its Correlation with Thermodynamic Data*. Pharm. Res., 1991. **8**: p. 1128-1136.
13. Byrn, S.R., P.A. Sutton, and B. Tobias, *The Crystal Structure, Solid-State NMR Spectra and Oxygen Reactivity of Five Crystal Forms of Prednisolone tert-butylacetate*. J. Am. Chem. Soc., 1988. **110**: p. 1609-1614.
14. Saindon, P.J., et al., *Solid-State Nuclear Magnetic Resonance (NMR) Spectra of Pharmaceutical Dosage Forms*. Pharm. Res., 1993. **10**: p. 197-203.
15. Suranarayanan, R. and T.S. Wiedmann, *Quantitation of the Relative Amounts of Anhydrous Carbamazepine and Carbamazepine Dihydrate in a Mixture by Solid-State Nuclear Magnetic Resonance*. Pharm. Res., 1990. **7**: p. 184-187.
16. Freeman, R., *A Handbook of Nuclear Magnetic Resonance*. 1988, New York: John Wiley and Sons Inc. 312.
17. Fyfe, C.A., *Solid State NMR for Chemists*. 1983, Guelph, Ontario, Canada: C.F.C. Press. 593.
18. Harris, R.K., *Nuclear Magnetic Resonance A Physicochemical View*. 1989, New York: John Wiley and Sons, Inc. 260.
19. Styles, P., et al., *A High-Resolution NMR Probe in Which the Coil and Preamplifier are Cooled with Liquid Helium*. J. Magn. Reson., 1984. **60**: p. 397-404.
20. Serber, Z., et al., *New Carbon-Detected Protein NMR Experiments Using CryoProbes*. Journal of the American Chemical Society, 2000. **122**(14): p. 3554-3555.



21. Shevgoor, S., et al. *Development of a CryoMAS(TM) HR-MAS-MAG NMR Probe for High-Field WB Magnets*. in *Experimental NMR Conference*. 2005. Providence, Rhode Island.
22. Oldfield, E., *A Multiple-Probe Strategy for Ultra-High-Field Nuclear Magnetic Resonance Spectroscopy*. J. Magn. Reson., Ser. A, 1994. **107**: p. 255-257.
23. MacNamara, E., et al., *Multiplex sample NMR: an approach to high-throughput NMR using a parallel coil probe*. Analytica Chimica Acta, 1999. **397**(1-3): p. 9-16.
24. Hou, T., E. MacNamara, and D. Raftery, *NMR Analysis of Multiple Samples Using Parallel Coils: Improved Performance Using Reference Deconvolution and Multidimensional Methods*. Anal. Chim. Acta, 1999. **400**: p. 297-305.
25. Fisher, G., et al., *NMR Probe for the Simultaneous Acquisition of Multiple Samples*. Journal of Magnetic Resonance, 1999. **138**(1): p. 160-163.
26. Hou, T., et al., *Analysis of Multiple Samples Using Multiplex Sample NMR: Selective Excitation and Chemical Shift Imaging Approaches*. Anal. Chem., 2001. **73**: p. 2541-2546.
27. Zhang, X., J.V. Sweedler, and A.G. Webb, *A Probe Design for the Acquisition of Homonuclear, Heteronuclear, and Inverse Detected NMR Spectra from Multiple Samples*. Journal of Magnetic Resonance, 2001. **153**(2): p. 254-258.
28. Raftery, D., et al., *Nuclear Magnetic Resonance of Multiple Samples*, in *US Patent and Trademark Office*. 2002: USA. p. 26.
29. MacNaughtan, M.A., et al., *High-Throughput Nuclear Magnetic Resonance Analysis Using a Multiple Coil Flow Probe*. Analytical Chemistry, 2003. **75**(19): p. 5116-5123.
30. Ike, et al., *NMR probe for multiplex resonance [Machine Translation]*, in *Jpn. Kokai Tokkyo Koho*. 2003, (Jeol Ltd., Japan). Jp. p. 7 pp.

## **Chapter 2**

### **Multiple-Sample Solid-State NMR Probe with Lumped-Element Tuning**

## 2.1 Introduction

As stated in the introductory chapter, solid-state NMR (ssNMR) of pharmaceutical compounds has not become a ubiquitous analytical technique due to the inherent cost of its lengthy experiments. This is unfortunate because to the ability of ssNMR to gain specific information about the structure and dynamics of a sample. If the number of samples analyzed per unit time were to be increase it may gain favor, enabling formulators to make better informed decisions about their compounds. Our approach to increasing sensitivity and throughput uses the fact that in ssNMR, the spin-spin relaxation time constant,  $T_2$ , is usually several orders of magnitude shorter than the spin-lattice relaxation time constant,  $T_1$ . [1] Figure 2.1 is a depiction of the relationship between the  $T_2$  related length of the free induction decay (FID), and  $T_1$  related pulse delay before acquisition of the next FID. The difference in relative magnitudes of  $T_2$  and  $T_1$  for solution NMR and ssNMR is also shown.

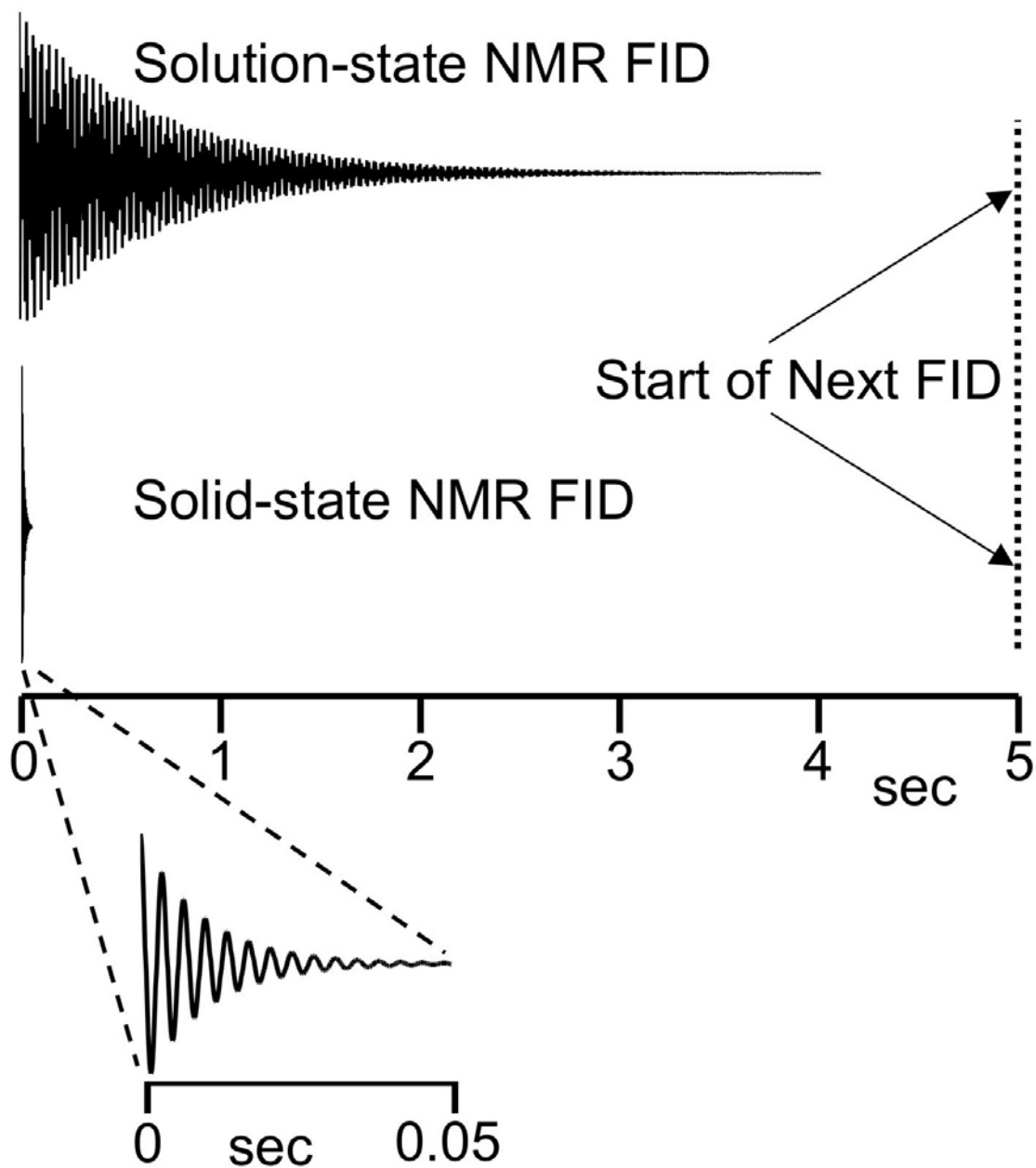


**Figure 2.1.** Graphical depiction of relative magnitudes of  $T_2$  and  $T_1$  for solution and solid-state NMR.

This short transverse relaxation time means that the preparation and acquisition time in a Fourier Transform ssNMR experiment is typically tens of milliseconds. Before the sample can be pulsed again, it must relax for several seconds to several hours as the bulk

magnetization returns to its equilibrium value. During this time the sample must remain in a strong static magnetic field, but is not required to be in a homogeneous magnetic field. We exploit this fact to increase sample throughput by shuttling multiple MAS systems through the magnet bore via physical translation of samples into and out of the homogeneous portion of the static magnetic field, where radio frequency (RF) pulse delivery and data acquisition occur.

## **2.2 Experimental**

### *2.2.1 Probe concept*

The basic probe design consists of multiple MAS systems that are located in the bore of the superconducting magnet dewar. One possible design of this probe is shown in Figure 2.2 where the MAS modules are aligned along the axis of the magnet solenoid.

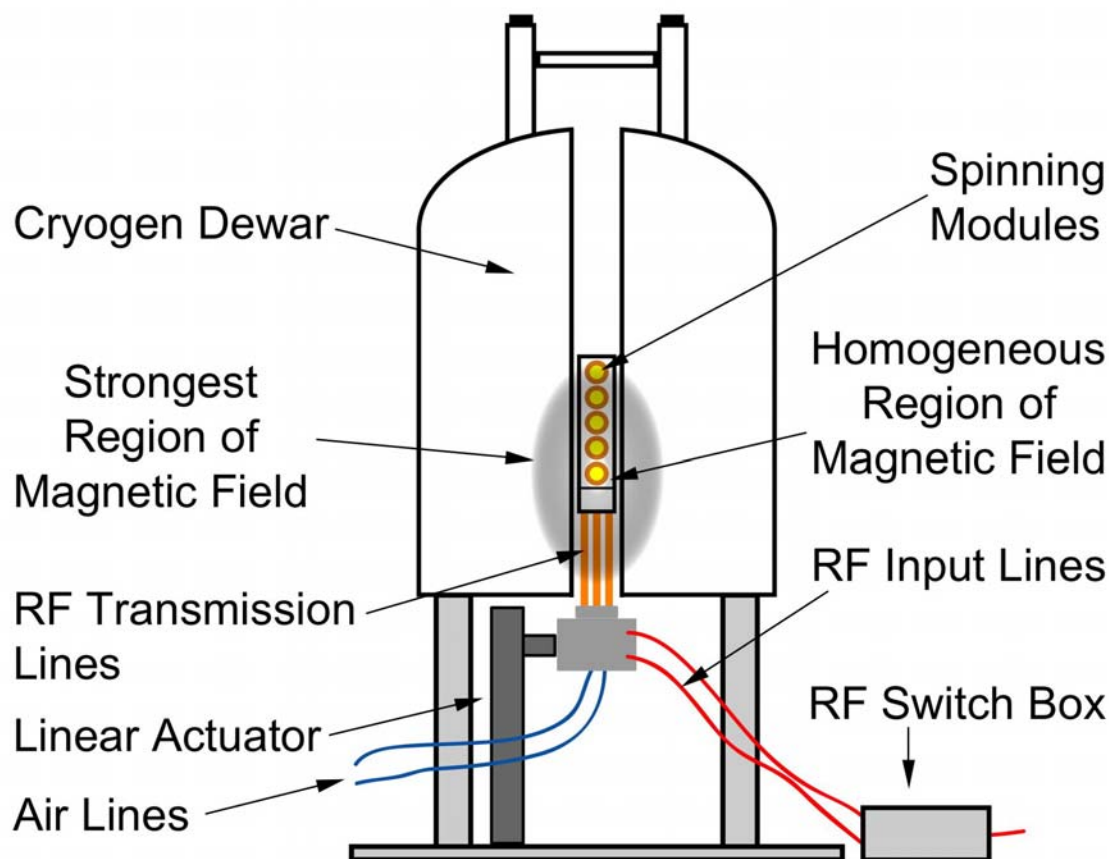
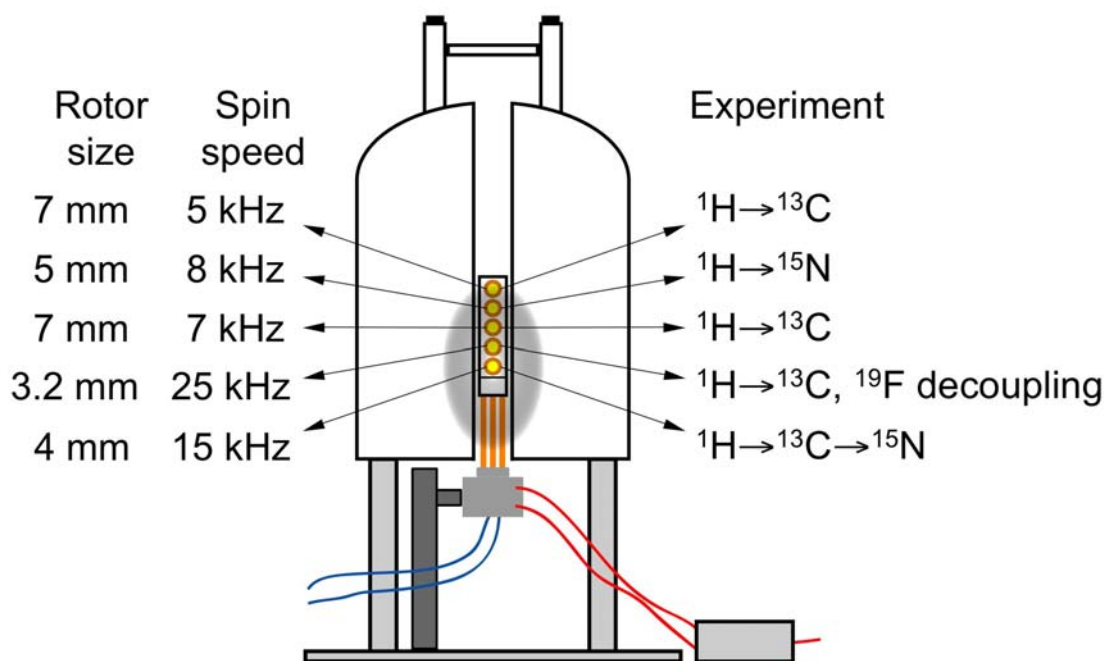


Figure 2.2. Basic concept for mss probe in the bore of the superconducting solenoid magnet.

The MAS modules can be moved into the homogeneous region of the magnet for signal acquisition. When the signal is not being acquired, the spinning systems may be moved into a non-homogeneous portion of the magnetic field. The MAS modules are moved in the bore of the magnet using an electric, hydraulic, or other mechanism that can change the location of the MAS modules in the magnet bore. In Figures 2.2 and 2.3, the concept of using a Linear Actuator assembly to move the probe in the magnetic field is shown. Ideally, each spinning system would feature its own air supply lines, radio-frequency (RF) connections, and magic-angle adjustment mechanism, although some or all of these features may be combined. In the design shown in Figure 2.2, there is a remote RF tuning and switching box that serves two purposes. First, each MAS module/circuit can be

selected independently for signal acquisition. Second, it allows each circuit to be tuned independently outside the bore of the magnet dewar. Each module may have various sized MAS modules, acquisition of various nuclei, independent spinning speed control, and independent shimming parameters. A potential arrangement is shown in Figure 2.3.



**Figure 2.3. Theoretical arrangement of MAS modules, spinning speeds, and experiments using one mss probe.** The samples would all be continuously spinning and each experiment would be conducted sequentially acquiring transients following translation into the homogeneous region of the field.

There are several advantages of this probe design. First, it has the capability of increasing throughput by a factor of 2–10, depending upon the number of spinning modules/samples that could be analyzed. This number could be significantly higher, if the analysis time for one sample was several days. During that time, the samples in the other spinning modules could be changed several times without disturbing the sample with the long analysis time. Moreover, this system has the capability of being automated, because the probe would be designed so that all of the MAS modules could be accessed from below the magnet. The throughput advantage could be increased to 10–50 compared

to a probe with no autosampler, if the samples were changed five times during an overnight run or over a weekend. If the choice is made to run the same sample nine times, then the SNR would be tripled. It would take nine times as long to triple the SNR by signal averaging using just one spinning module. Moreover, there should be little or no loss in field homogeneity, sensitivity, MAS speed, or  $^1\text{H}$  decoupling field strength compared to conventional NMR probes, nor is there a need to develop specialized spinning modules, pulse sequences, or RF technology. While this approach can be used at any magnetic field strength, it would work better at higher field strengths, where  $T_1$  relaxation rates are much longer than at lower field strengths.[2] Higher fields also imply faster spinning systems and therefore smaller sample volumes and MAS modules. This would mean that more spinning systems could be placed in the static magnetic field, enabling more samples to be run.

There are practical limitations to this approach. For example, this probe design is not as useful for studying nuclei in samples that have short relaxation times, such as many quadrupolar nuclei. Also, additional sample is needed if an increased SNR is desired. The modules would be self-contained, which could limit the experiments to fixed angle, double resonance, and room temperature. The constant moving of the probe may make it more prone to mechanical breakdown, and the multiple spinning modules/circuits will increase maintenance problems. Finally, having multiple spinning modules will require significantly more compressed air and plumbing for delivery of air to each MAS module. All of these limitations are relatively minor compared to the gains in throughput/sensitivity that would be achieved with this probe.



### 2.2.2 Effect of Magnetic Field Strength along Superconducting Solenoid Axis

The magnetic field of NMR magnets is generated by the precession of electrons in wires of a solenoid. The solenoid is immersed in liquid helium so that the nickel-cadmium wires may become superconducting. The ideal superconducting magnet for the multiple-sample probe would have a magnetic field strength that remained approximately constant for as long as possible along the axis of the solenoid. A diagram of the field strength for an Oxford (Oxford, UK) 9.4 Tesla, 89 mm bore magnet with 7 MAS modules in various positions is shown in Figure 2.4.

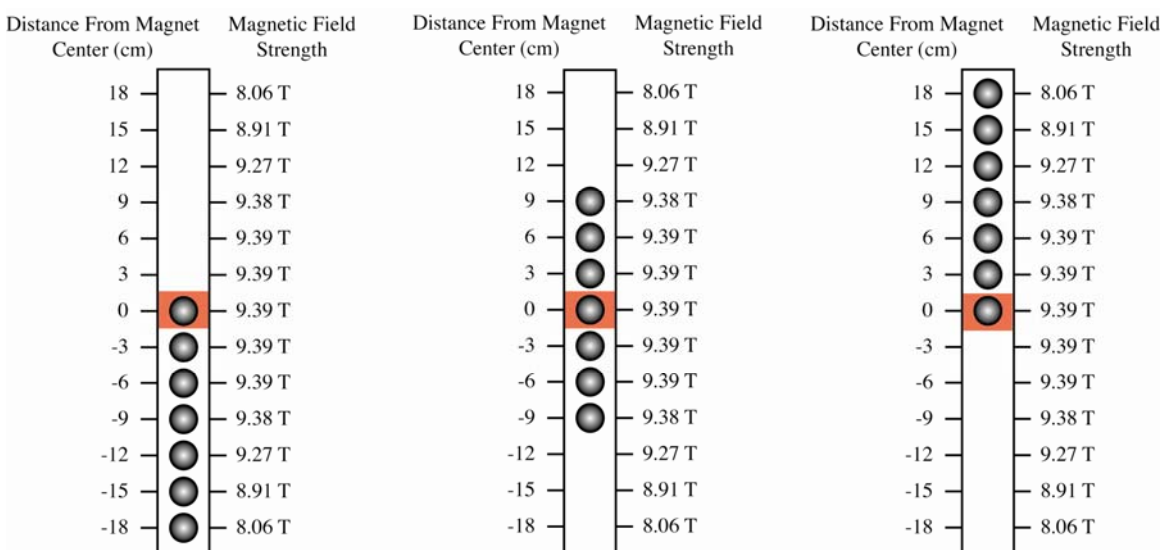


**Figure 2.4. Diagram of different positions of MAS modules in the bore of a 9.4 Tesla superconducting magnet.** The homogeneous region of the field, where data acquisition occurs, is highlighted in red. Each MAS module is shown as a grey sphere.

The effective field, defined as the point at which the field remains greater than 80%, is approximately 18 cm from the center of the solenoid. If all samples were confined to an 18 cm range, then only the two outer samples would feel a magnetic field of less than 95%, and then only while one of the outer samples was being analyzed.

A two-sample probe based upon a lumped element (Hester-Waugh)[3] tuning circuit was developed to test the feasibility of multiple-sample probe technology. A picture of the probe is shown in Figure 2.5.

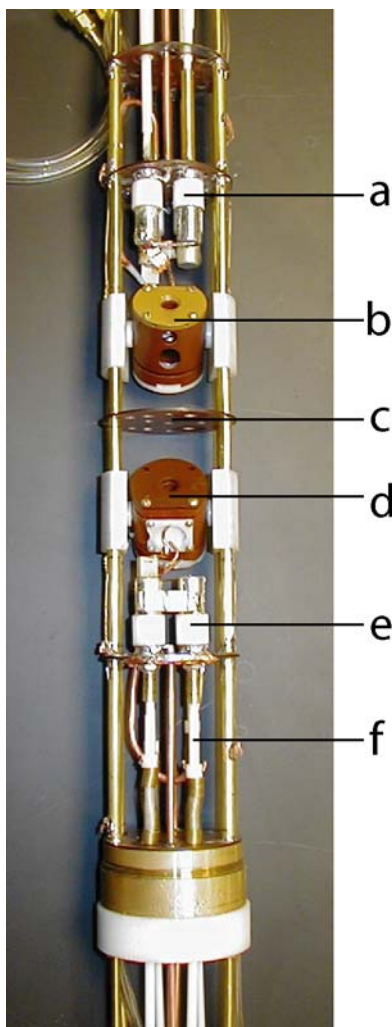


**Figure 2.5. Picture of multiple-sample probe with lumped element (Hester-Waugh) tuning circuits.** (a) top tuning circuit, (b) top MAS module, (c) RF isolation plane, (d) bottom MAS module, (e) bottom tuning circuit, (f) tuning wands

The probe is designed with an axis of symmetry to facilitate construction. There are four main components of the probe: MAS modules, air lines, tuning circuits, and RF transmission lines. Standard Varian (Palo Alto, CA) 7.5 mm spinning modules were used. The modules are ~1.5" in diameter and spin 7.5 mm rotors up to 7000 Hz. Flexible

plastic tubing, 1/8" i.d., supplies compressed air to Delrin® plastic supports. The Delrin® supports hold the spinning module in place and deliver the compressed air to the drive and bearing systems. The tuning circuit is comprised of several elements based on the Hester-Waugh[3] design. The coil is made from four turns of 16 gauge solid copper wire. American Technical Ceramics (Huntington Station, NY) fixed capacitors, and Polyflon variable capacitors (Norwalk, CT) are used to match and tune the circuit. A quarter wavelength isolation element was made by using 1/2" copper pipe and 3/16" solid copper wire to complete the tuning circuit. Tuning wands made of mixed plastic and brass parts are used to adjust the variable capacitors from outside the magnet. RF power is supplied to the tuning circuit via 1/8" semi-rigid copper coaxial cable.

Figure 2.6 shows a photograph of the two-module probe in the bore of the superconducting magnet dewar.

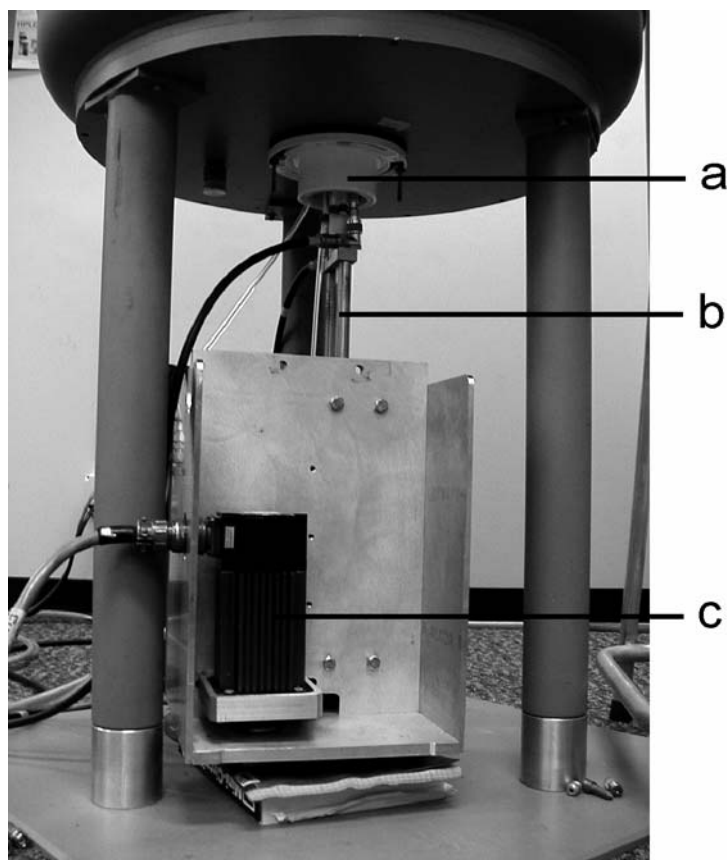


**Figure 2.6. Photograph of probe in magnet.** The probe is moved using a stepper motor assembly: (a) probe guide in magnet, (b) probe movement assembly, (c) stepper motor.

A PVC probe guide is used to avoid having the probe body rub against the magnet bore while moving. An Emerson Electric Co. (St. Louis, MO) model DXM-138 stepper motor, controlled via model MO35138 controller, is attached via pulley to a worm screw. The worm screw is able to raise/lower the assembly (shown in Figure 2.6-b) approximately 20 cm. Operation of the stepper motor under the magnet had no noticeable effect on the spectra.

The samples in the MAS modules were located  $\sim 12$  cm apart in the probe. When the top module was located in the homogeneous region of the magnet, it took  $\sim 1$  s to move the bottom module into the homogeneous region of the magnet. For some reason, possibly related to the controller software, it took  $\sim 2$  s to move the opposite direction. A

PC running a Microsoft Excel macro was used to control movement height and speed. Although it is possible to interface the movement control to the spectrometer hardware, the difficulty in synchronizing the two programs prompted us to delay interfacing until a new motor/controller and spectrometer console arrived.

### *2.2.3 Solid-State NMR Spectra*

All spectra were acquired using a Chemagnetics (Fort Collins, CO) CMX-II SSNMR spectrometer equipped with a Magnex 300 (Yarnton, UK) superconducting magnet operating at 75.6 MHz for  $^{13}\text{C}$ . Samples were spun at the magic angle at a rate of  $\sim 3000$  Hz. Variable-amplitude cross polarization (VACP)[4, 5] was used to acquire all spectra. Proton decoupling powers of 40-80 kHz were used to acquire all spectra. Acquisition parameters for hexamethylbenzene (HMB) were: 512 data points, 30 kHz spectral width, and 17 ms acquisition time. All spectra were zero-filled to 4096 points prior to Fourier transform. No apodization was used. SNR measurements of HMB spectra were made by using a macro feature of the Spinsight software. Noise was sampled over a 30 ppm chemical shift range. Signal intensity was determined from the methyl peak of HMB. SNR was reproducible within 5% on consecutive acquisitions.

## **2.3 Results**

The spectra of HMB acquired in both the top and bottom spinning modules are shown in Figure 2.7.

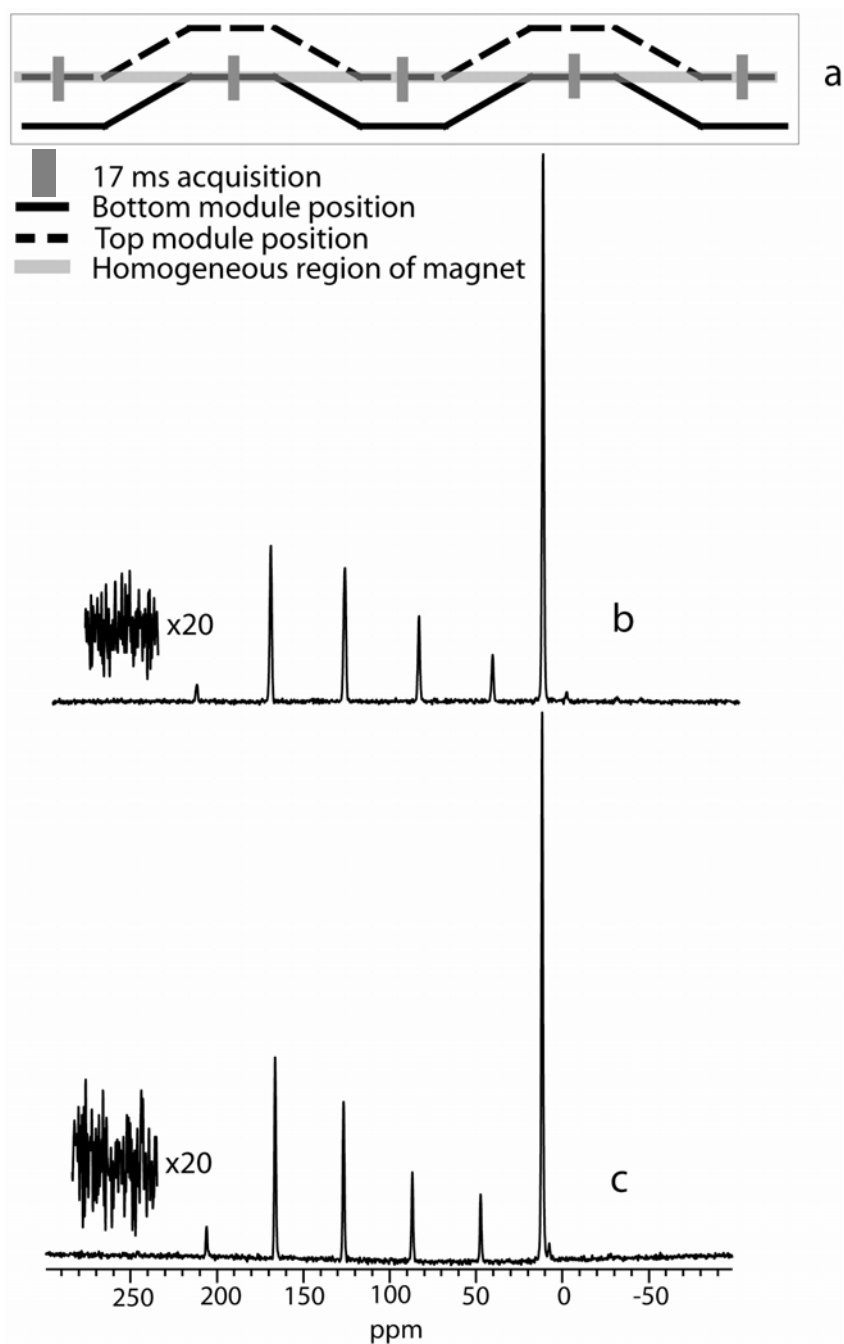


**Figure 2.7. HMB  $^{13}\text{C}$  spectra acquired from top and bottom module.** Each spectrum was 12 acquisitions and each acquisition was alternated between the modules: (a) schematic of module position in magnet and pulse timing, (b) spectrum acquired in top module, (c) spectrum acquired in bottom module.

The SNR for the top module was  $\sim 320$ , which is comparable to that observed using our conventional probes at the time. The SNR of the bottom module was  $\sim 250$ . The reduced SNR probably reflects poor RF shielding. The  $^1\text{H}$   $90^\circ$  pulse widths for both modules was

$\sim 4.0 \mu\text{s}$ . The spectra in Figure 2.7 were acquired by alternating each acquisition between the top and bottom module, showing that it is possible to return each module in the probe to the homogeneous region of the magnet.

Figure 2.8 shows a spectrum of HMB acquired using the bottom module.

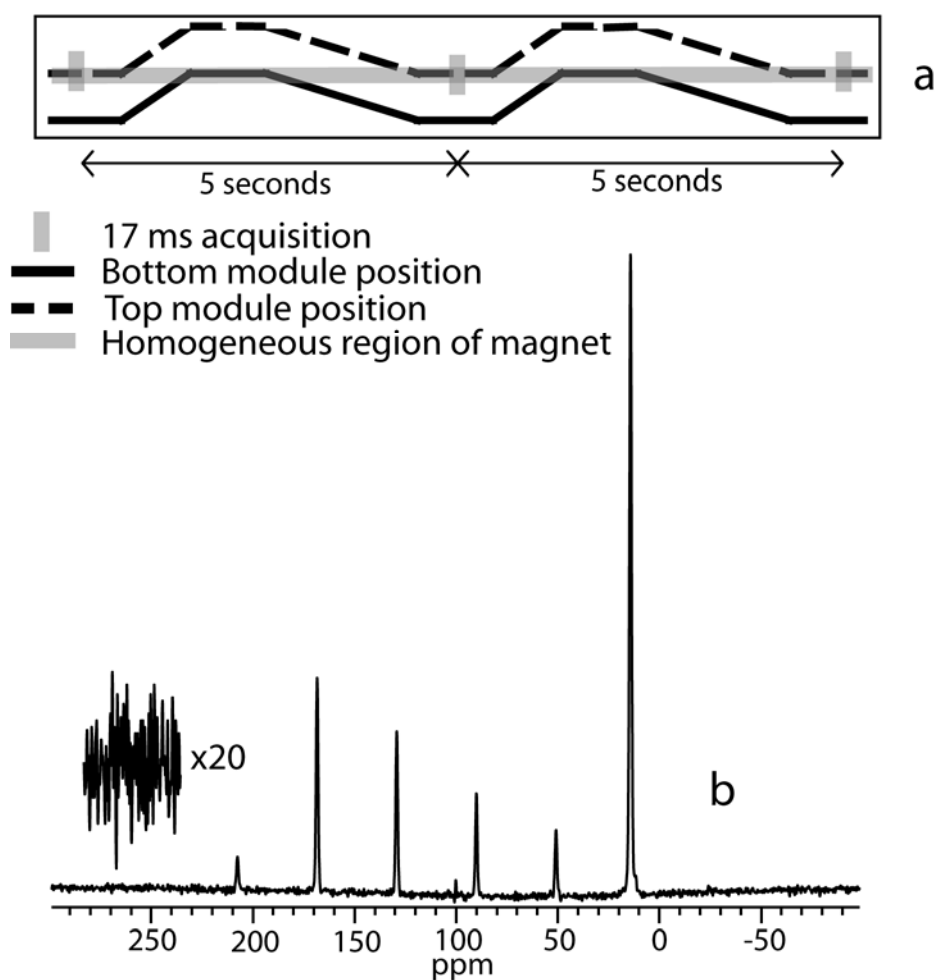


**Figure 2.8.**  $^{13}\text{C}$  spectrum of HMB acquired using the bottom module with the pulse sequence timing chosen to coincide with probe movement. (a) schematic of timing of probe movement and spectral acquisition, (b) HMB spectrum.

The purpose of this experiment was to synchronize the acquisition with the movement. The schematic in Figure 2.8-a shows the timing sequence of the movement and the spectral acquisition. It was determined that the following cycle took 4.8 s, where the order refers to which sample is in the homogeneous region of the magnet: bottom

module (1 s), move to top (1 s), top module (1 s), move to bottom module (2 s). Because the movement was very reproducible, spectral acquisition with a 4.8 s repetition time between pulses was used, starting with the bottom module in the homogeneous region of the magnet. The HMB spectrum obtained is comparable to one acquired without movement.

Figure 2.9 shows the  $^{13}\text{C}$  CPMAS NMR spectra of aspirin and ibuprofen. Crystalline aspirin has a  $^1\text{H}$   $T_1$  of  $\sim 30$  s at 7.05 T. To obtain quantitative spectra, which is often important for solid pharmaceuticals, a relaxation delay of 5 times  $T_1$  must be used. For this experiment a 90 s delay was used, and 64 transients were acquired (Figure 2.9-b). The spectrum of aspirin in the top module is shown in Figure 2.9-a. During the delay the top module was moved out of the homogeneous region of the magnetic field, and the bottom module, containing ibuprofen, was moved into the homogeneous region. Thirty transients of ibuprofen using a 3 s recycle delay were acquired before moving the top module back into the homogeneous region of the magnet. A total of 1920 transients were acquired on ibuprofen, while the 64 were acquired on the aspirin sample. The combined analysis obtained in this interleaved approach yielded a time savings of 1.5 hours.



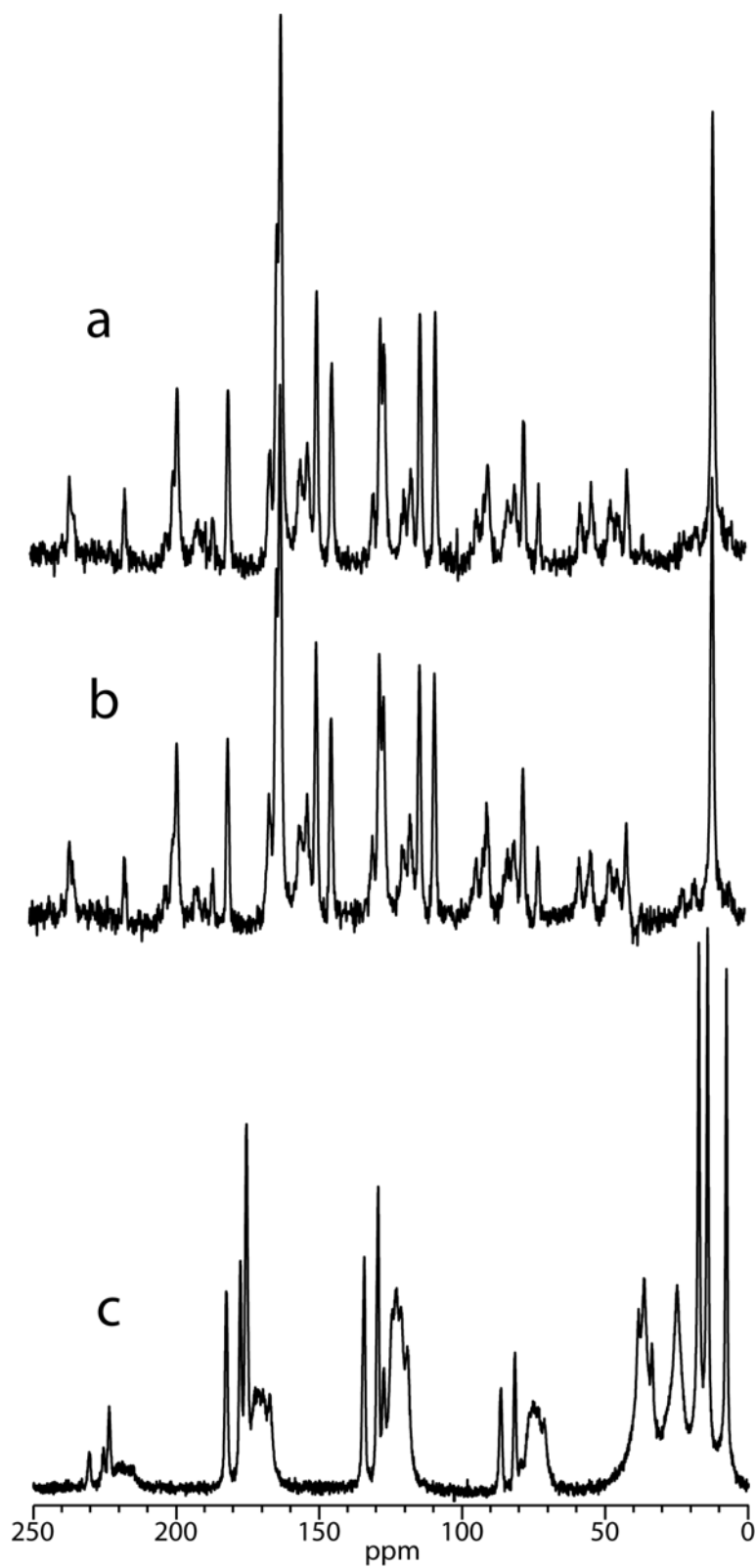


**Figure 2.9.**  $^{13}\text{C}$  spectra of aspirin and ibuprofen. (a) aspirin acquired without motion, (b) aspirin acquired with motion and switching, (c) ibuprofen acquired with motion and switching.

Several interesting features can be observed from the spectra in Figure 2.9. First, the spectra of aspirin acquired with and without movement are indistinguishable. Second, the field at which the aspirin was located while the spectrum of ibuprofen was acquired must have been very close to 7 T in order for the Boltzmann population difference to return to the same value as in the spectrum acquired without movement. Finally, the concept of sample shuttling as a method of simultaneous acquisition in a superconducting magnet has been demonstrated.

## 2.4 Conclusion

In this chapter we showed that the ability to acquire CPMAS spectra of two samples simultaneously is possible. The spectra are high quality, with SNRs comparable to conventional probe technology. Shuttling of MAS modules sequentially into the homogeneous region of the magnet does not reduce spectral quality, while saving substantial amounts of time. Although we have only shown applications of this probe design to pharmaceuticals, it could also benefit researchers in fields such as glasses, catalysis, and polymers.

## 2.5 References

1. Fyfe, C.A., *Solid State NMR for Chemists*. 1983, Guelph, Ontario, Canada: C.F.C. Press. 593.
2. Harris, R.K., *Nuclear Magnetic Resonance A Physicochemical View*. 1989, New York: John Wiley and Sons, Inc. 260.
3. Cross, V.R., R.K. Hester, and J.S. Waugh, *Single Coil Probe with Transmission-line Tuning for Nuclear Magnetic Double Resonance*. Review of Scientific Instruments, 1976. **47**(12): p. 1486-1488.

4. Peersen, O.B., et al., *Variable-Amplitude Cross-Polarization MAS NMR*. Journal of Magnetic Resonance Series A, 1993. **104**(3): p. 334–339.
5. Pines, A., M.G. Gibby, and J.S. Waugh, *Proton-enhanced NMR of Dilute Spins in Solids*. Journal of Chemical Physics, 1973. **59**(2): p. 569–590.

## **Chapter 3**

### **Multiple-Sample Solid-State NMR Probe with Three-Quarter Wavelength Coaxial Transmission Lines**

### 3.1 Introduction

The next step in developing a practical multiple-sample probe was designing an MAS module and tuning circuit that could accommodate six or more samples. Various concepts were evaluated based upon the Hester-Waugh design, but the disadvantage of that design is the necessity of having 24 tuning wands, 12 air lines, and 12 RF coaxial cables emerging from the bottom of the probe. In addition, four variable capacitors, several fixed capacitors, and one  $\lambda/4$  transmission line isolation element would have to exist between each module. During this evaluation process we began to consider the McKay  $\lambda/4$  transmission design. A detailed description of this probe design can be found in Stejskal and Memory,[1] and a schematic of the circuit is shown in Figure 1.2. This probe design was commercialized by Chemagnetics in the late 1980s, and is still used in our laboratory. In the Chemagnetics probe, the transmission line is  $\sim 4$  cm in diameter, with the  $\lambda/4$  tap point for the X nucleus located approximately at the midpoint of the transmission line. The advantage of this probe design is that the tuning elements are all located outside the magnet bore, and the only RF connection between the module and the tuning elements is the transmission line.

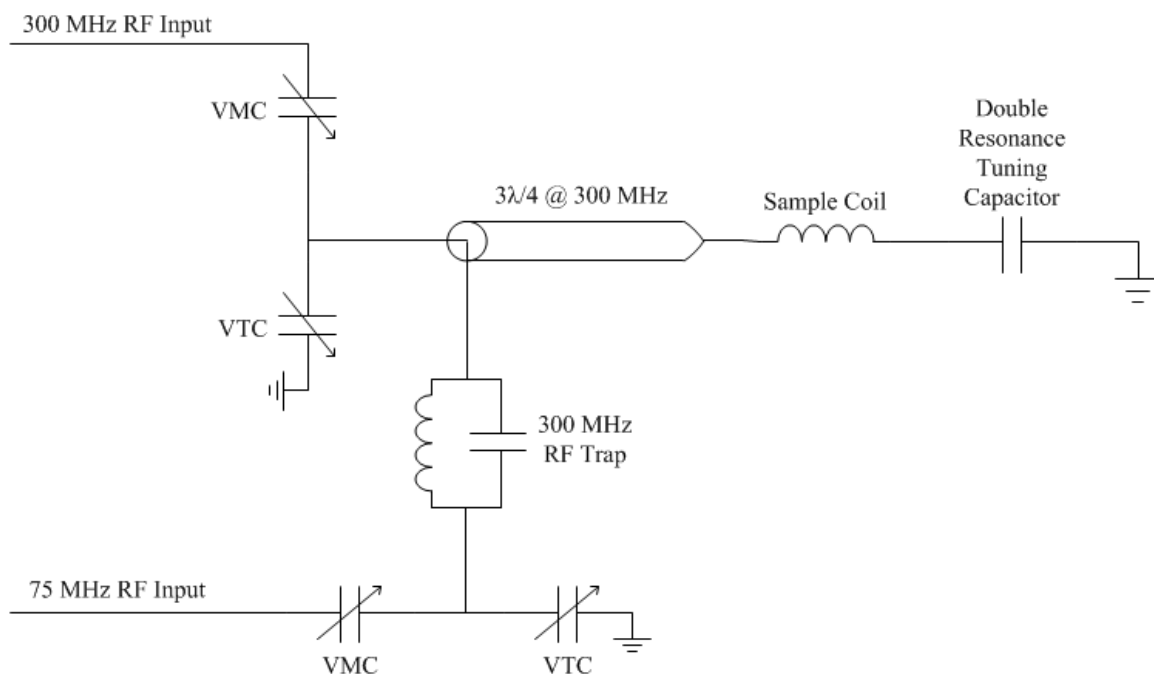


**Figure 3.1.** Tuning circuit for a  $3\lambda/4$  transmission line double resonance NMR probe (VMC and VTC are Variable Match and Tune Capacitors).

At a  $^1\text{H}$  frequency of 300 MHz, the transmission line extends out of the magnet just enough to be tuned with a capacitor. Our concern was that all of the tuning elements for a six module probe could not be outside the magnet bore, due to the extra length of transmission line required to reach the top module. As such, rather than using a  $\lambda/4$  design, we chose a  $3\lambda/4$  design. The tuning circuit, shown in Figure 3.1, is the same as shown in Figure 1.1 with a  $3\lambda/4$  transmission line in place of the  $\lambda/4$  transmission line. Transmission line design theory, discussed in the introduction chapter, states that a  $\lambda/4$  and  $3\lambda/4$  should be equivalent in terms of tuning elements. The extra length of a  $3\lambda/4$  design would allow all of the tuning elements to be located outside the magnet. The disadvantage of the  $3\lambda/4$  design is that the RF performance may suffer, especially since the transmission line diameter must be decreased to less than 2.5 cm to accommodate more MAS modules.

A  $3\lambda/4$  probe was constructed to test the performance of the proposed tuning circuit. The transmission line from an unused Chemagnetics  $\lambda/4$  probe was replaced with a Dielectric Communications (Raymond, ME) 7/8" o.d. air dielectric transmission line with a tap point at the  $3\lambda/4$ . A picture of the  $3\lambda/4$  probe is shown in Figure 3.2. The Varian 7.5 mm MAS module was replaced with a 7 mm MAS module purchased from Revolution NMR (Fort Collins, CO). This new module has a considerably smaller outside diameter ( $\sim 2$  cm) compared to the module used in the previous probe ( $\sim 4$  cm). Both modules are pictured in Figure 3.3. A smaller MAS module diameter is critical to be able to space the modules as closely as possible. The probe was configured for  $^{13}\text{C}$ - $^1\text{H}$  double resonance by soldering an appropriate capacitor between one coil lead and ground. The only probe elements extending from the base of the probe to the MAS module are the transmission line, drive and bearing gas lines, and magic-angle adjustment. Because both the center and outer conductors of the transmission line are hollow, it is possible to divert the gases for spinning through the transmission line, saving additional space in the probe.



**Figure 3.2. Picture of  $3\lambda/4$  transmission line probe.** The tuning elements located in the silver circular portion on the left and the copper transmission line leading to the MAS module on the right. Also pictured are the air lines for MAS made of clear plastic tubing and brass couplers.

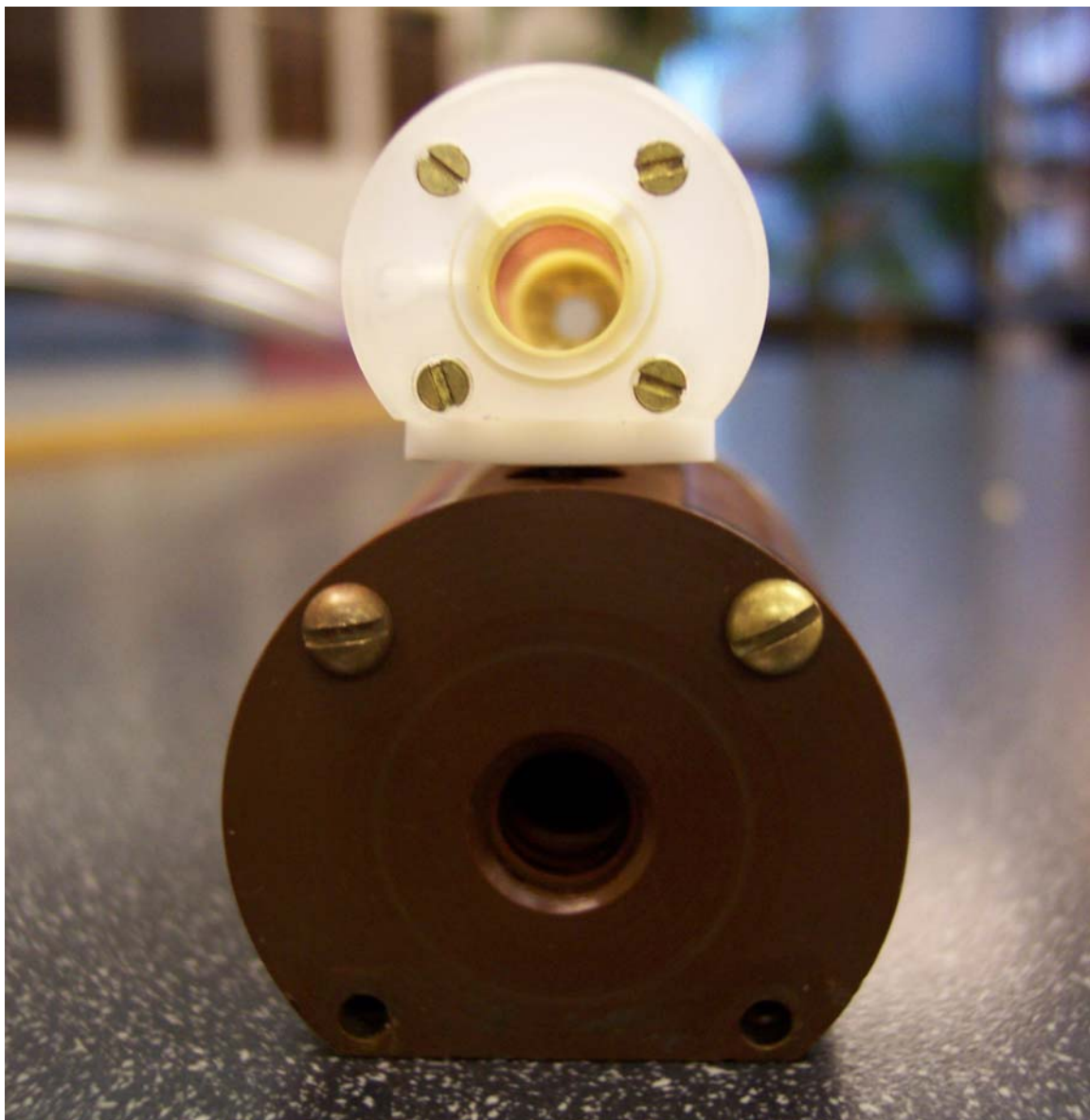


**Figure 3.3. Picture of Revolution NMR (top) and Varian (bottom) MAS modules, which illustrates the factor of 2 differences in module diameter.**

Table 3.1 shows the RF performance of the  $3\lambda/4$  probe for various numbers of coil turns. The performance of a conventional probe equipped with a Varian 7.5 mm MAS module and equivalent amount of sample in the rotor is shown for comparison. Different numbers of coil turns were evaluated when it was determined that the original coil design, which was a 6-turn coil, had a very poor SNR.



**Table 3.1. 90° pulse width and SNR of various coils in 1/4  $\lambda$  and 3/4  $\lambda$  probes.**

Turns in Coil	90° Pulse Width ( $\mu$ s)	SNR
6 (1/4 $\lambda$ )	3.8	348
6 (3/4 $\lambda$ )	2.9	257
7 (3/4 $\lambda$ )	3.2	354
8 (3/4 $\lambda$ )	3.6	368
9 (3/4 $\lambda$ )	3.8	423

The data in Table 3.1 clearly shows that the 3 $\lambda$ /4 probe can deliver improved SNR with effective  $^1\text{H}$  decoupling fields ( $> 60$  kHz) compared to current  $\lambda$ /4 probe technology in our laboratory. The primary disadvantage of the probe was that additional decoupling power ( $\sim 2\times$ ) was required to achieve the equivalent  $^1\text{H}$  decoupling field found on the commercial probe. However, no RF breakdown (i.e. arcing) was observed with the 3 $\lambda$ /4 probe at the higher power levels used, attesting to the robustness of the probe design. Given the relative simplicity of the design with only a transmission line, MAS module, one single fixed capacitor, and magic-angle adjustment in the magnet bore, expanding this to accommodate multiple MAS modules should be straightforward. Moreover, the design allows for remote tuning of the circuit outside the magnet bore.

## **3.2 Experimental**

### *3.2.1 Probe Construction*

After some two module mss probes where constructed and preliminarily tested, a design with four modules was settled upon. Four modules provides a good balance between effectively taking advantage of pulse delay instrument dead time and mechanical space available. The design of the four-module probe is shown in Figures 3.4 and 3.5.

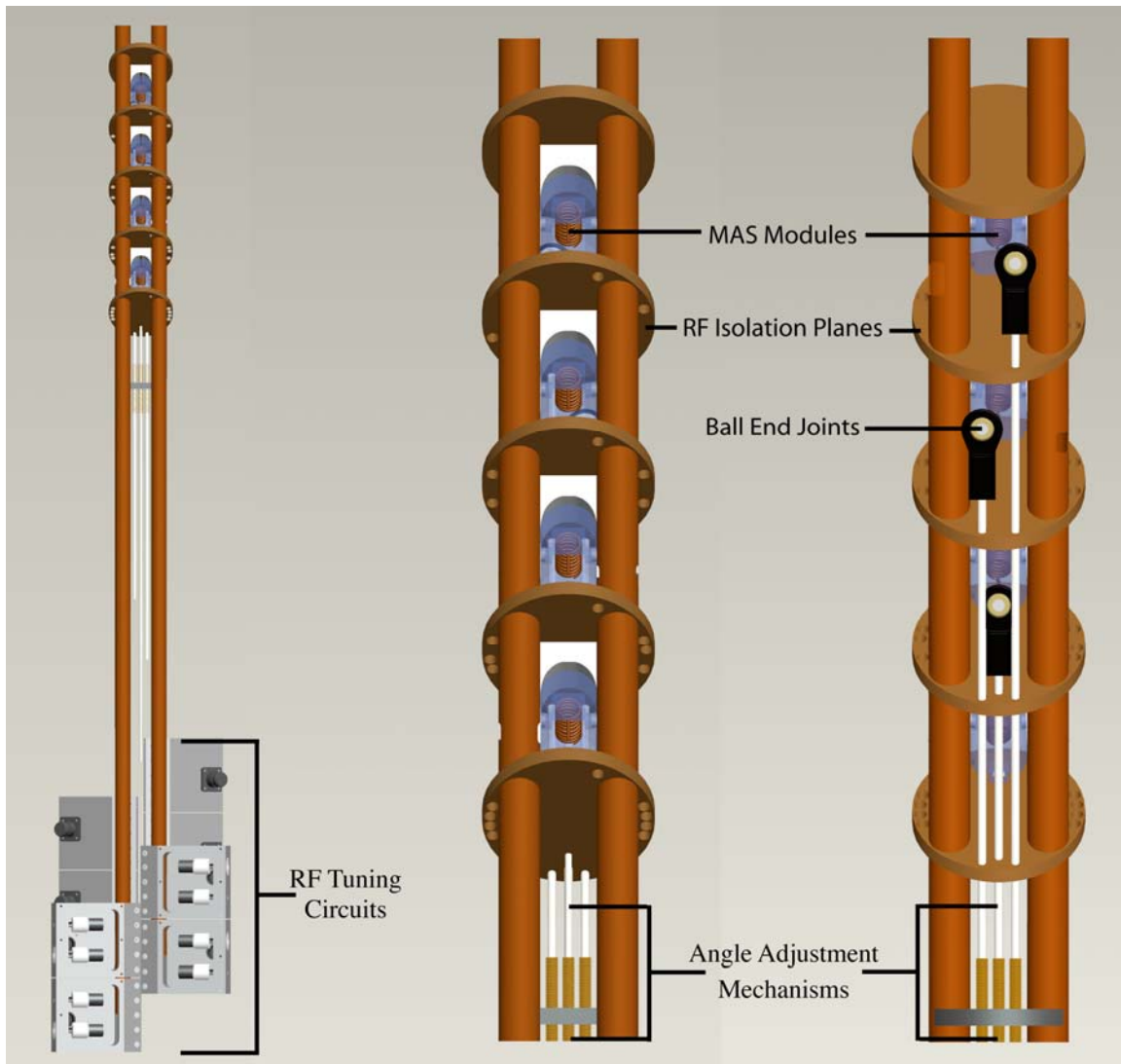


**Figure 3.4. Principle views of mechanical engineering assembly of the 4-module mss probe.** From Left: Full Length View; Top Section Front and Rear Views.

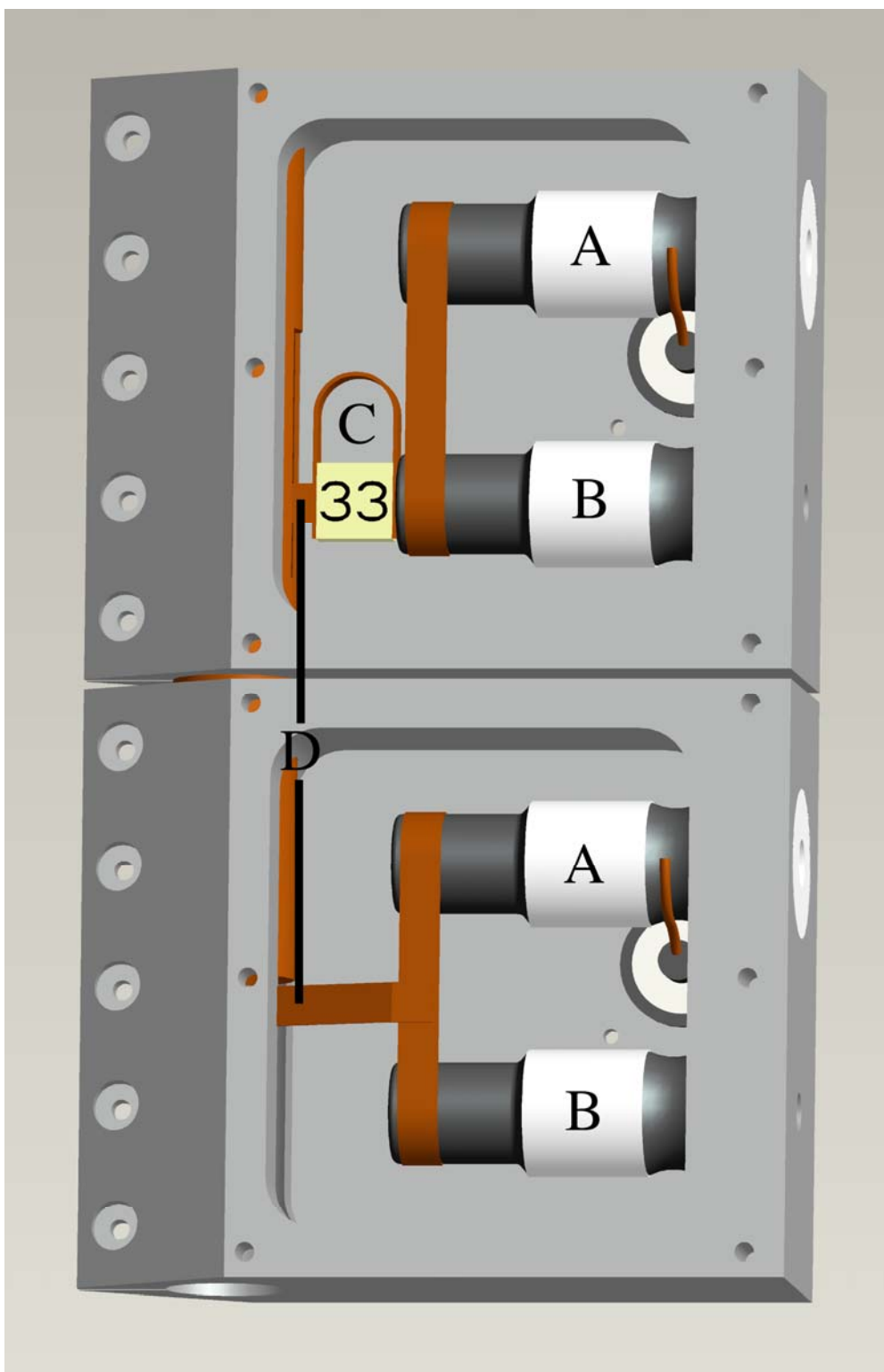


**Figure 3.5. Design of X (top) and H (bottom) tuning circuits.** A) Variable Match Capacitors; B) Variable Tune Capacitors; C)  $^1\text{H}$  RF Trap; D) Copper Leads to Transmission Line Center Conductor.

The transmission lines outer conductors are 5/8" copper tubing, and the inner conductors are 3/16" which have a calculated characteristic impedance of 67  $\Omega$ . Air is the dielectric for ~95% of the length, and small Teflon dielectrics are used to center the conductors relative to one another. These transmission lines were more efficient conductors of RF in the probe than the 50  $\Omega$  conductors in the single module prototype. Copper clad fiberglass circuit boards provide RF isolation planes between MAS modules. Flexible plastic tubing (1/8" i.d.) supplies compressed air to the bearing and drive systems of the MAS modules. Mixed plastic rods are used as magic angle adjustment rods with brass or aluminum 10-32 threaded rod for actuation. Mixed plastic ball end joints facilitate conversion of linear motion of the angle adjustment rods and circular motion of the MAS modules. Tuning circuit boxes are made of aluminum and have stainless steel screws to provide clamping force to the transmission lines. The sample coils are made of eleven turns of 16 gauge copper wire in a diameter providing minimal clearance for the sample rotor. Tuning of the circuits is done with variable capacitors from Polyflon (Norwalk, CT) and fixed capacitors from American Technical Ceramics (ATC) (Huntington Station, NY). A RF trap constructed of a 33 pF ATC capacitor and copper induction loop provides isolation of the  $^1\text{H}$  circuit from the X circuit. An Adept Technology, Inc. (Pleasanton, CA) Smart Axis linear actuator moves the probe vertically in the magnet bore. JFW Industries (Indianapolis, IN) high power solid-state RF switches were used to select probe channels.

### 3.2.2 Solid-State NMR Spectra

All spectra were acquired using a Tecmag (Houston, TX) Apollo ssNMR spectrometer equipped with a Oxford (Oxford, UK) 89 mm bore superconducting magnet operating at 75.9 MHz for  $^{13}\text{C}$ . Samples were spun at the magic angle at a rate of 3 to 4 kHz and were independently controlled via spin speed controllers from Revolution NMR, LLC (Fort Collins, CO). Ramped cross polarization[2] was used to acquire all spectra. Proton decoupling powers of 40-80 kHz were used to acquire all spectra.

Acquisition parameters for methylglutaric acid (MGA) were: 3072 data points, 103 ms acquisition time, and zero filled to 32,768 points prior to Fourier transform (FT). Acquisition parameters for adamantane were: 5120 acquisition points, 172 ms acquisition time and zero filled to 65,536 points prior to FT. All spectra were collected with a 30 kHz spectral width. No apodization was used. Signal to noise ratio (SNR) measurements of HMB and MGA spectra were made by using a noise window sampled over a 30 ppm chemical shift range, and signal intensity was determined from the methyl peak of each. SNR was reproducible within 5% on consecutive acquisitions. Determination of MAS module position in a homogeneous region of the super conducting magnet was performed using adamantane line widths. The setting of the magic angle was facilitated by monitoring the acid peaks (181.15 ppm) of MGA, which have baseline resolution when the proper angle is reached.[3]

## 3.3 Results

Linear actuator positioning for each module was done by collecting spectra of adamantane. The heights of the modules were jogged in small increments until line

widths were minimized, and the position was then stored to the Smart Axis position table. MGA was used to set the magic angle and calculate the SNR of each module. During these SNR measurements it was found that the solid-state switches were lossy. Without the switches in the circuit the SNR of MGA was 20% higher, and comparable to that of conventional probe technology.

Acquisition of MGA in all four modules was accomplished in the same amount of time required for one MGA spectrum in a conventional probe. Because of the limitations of the pulse sequencing of the NTNMR software on the Tecmag spectrometer, during collection of the multiple spectra the free induction decay (FID) of each sample is continuously plotted as show in Figure 3.6. Upon completion of acquisition the FIDs are separated and FT is applied to produce the individual spectra shown in Figure 3.7.

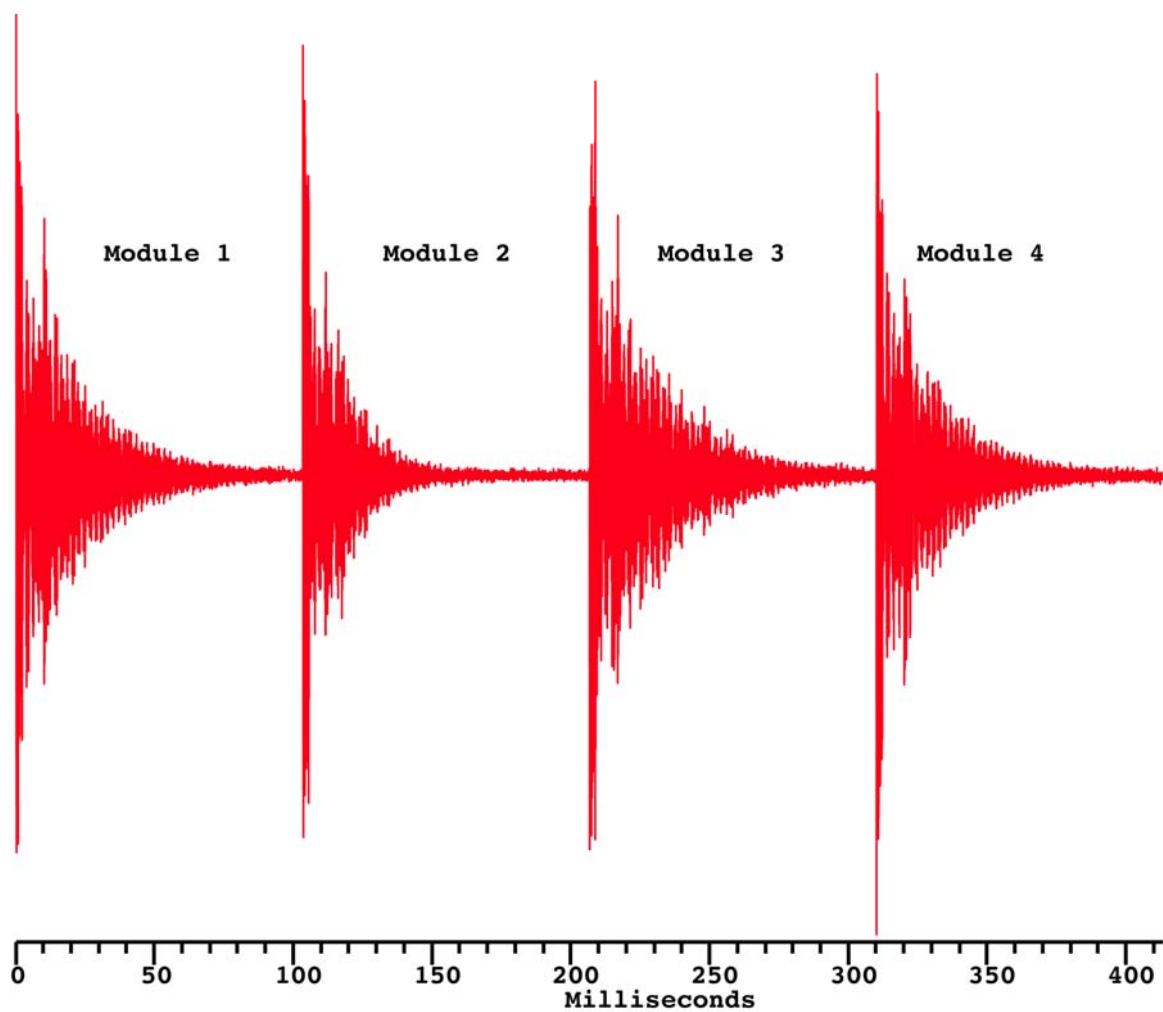


Figure 3.6. FID of MGA in all modules of mss probe.

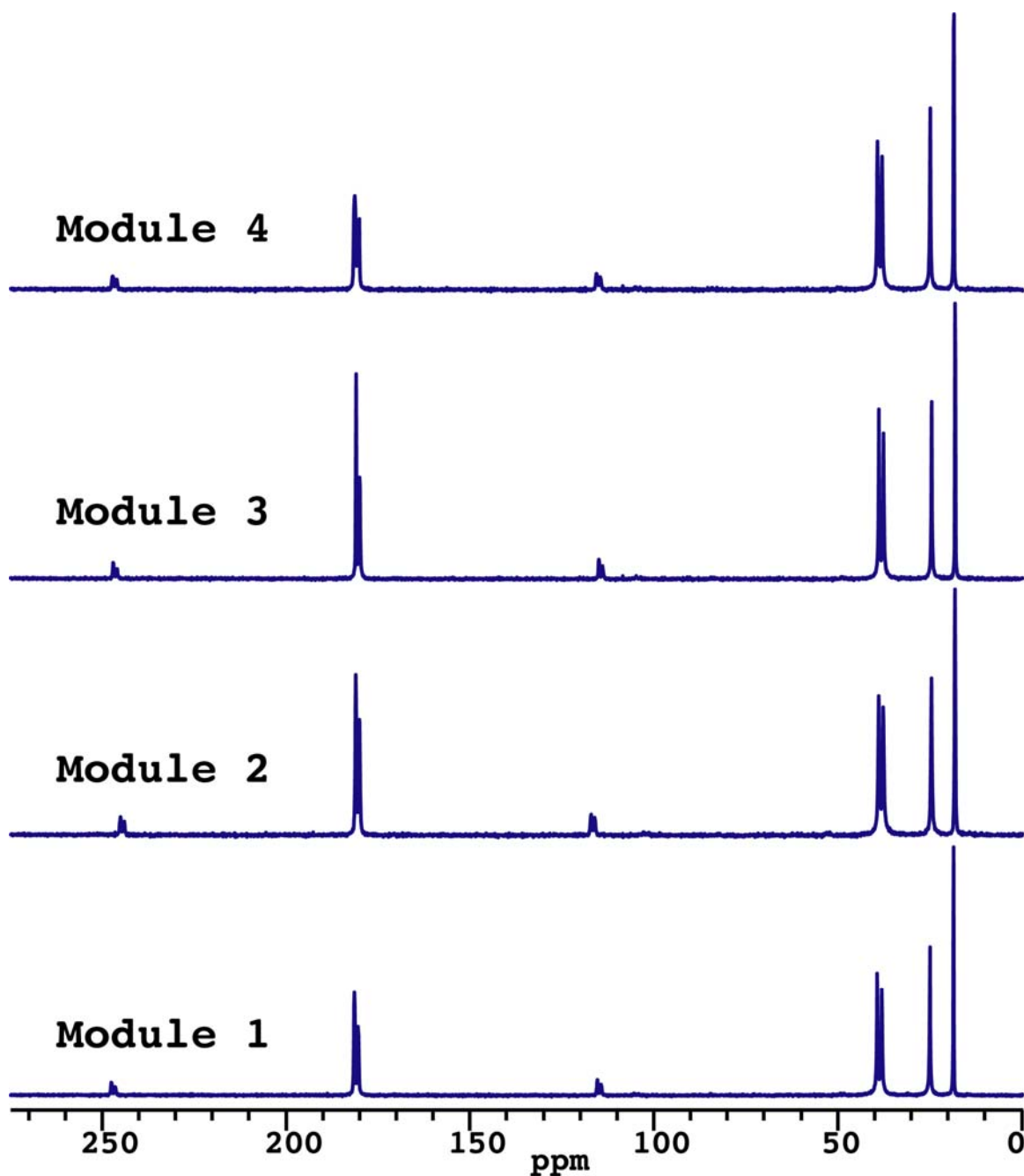
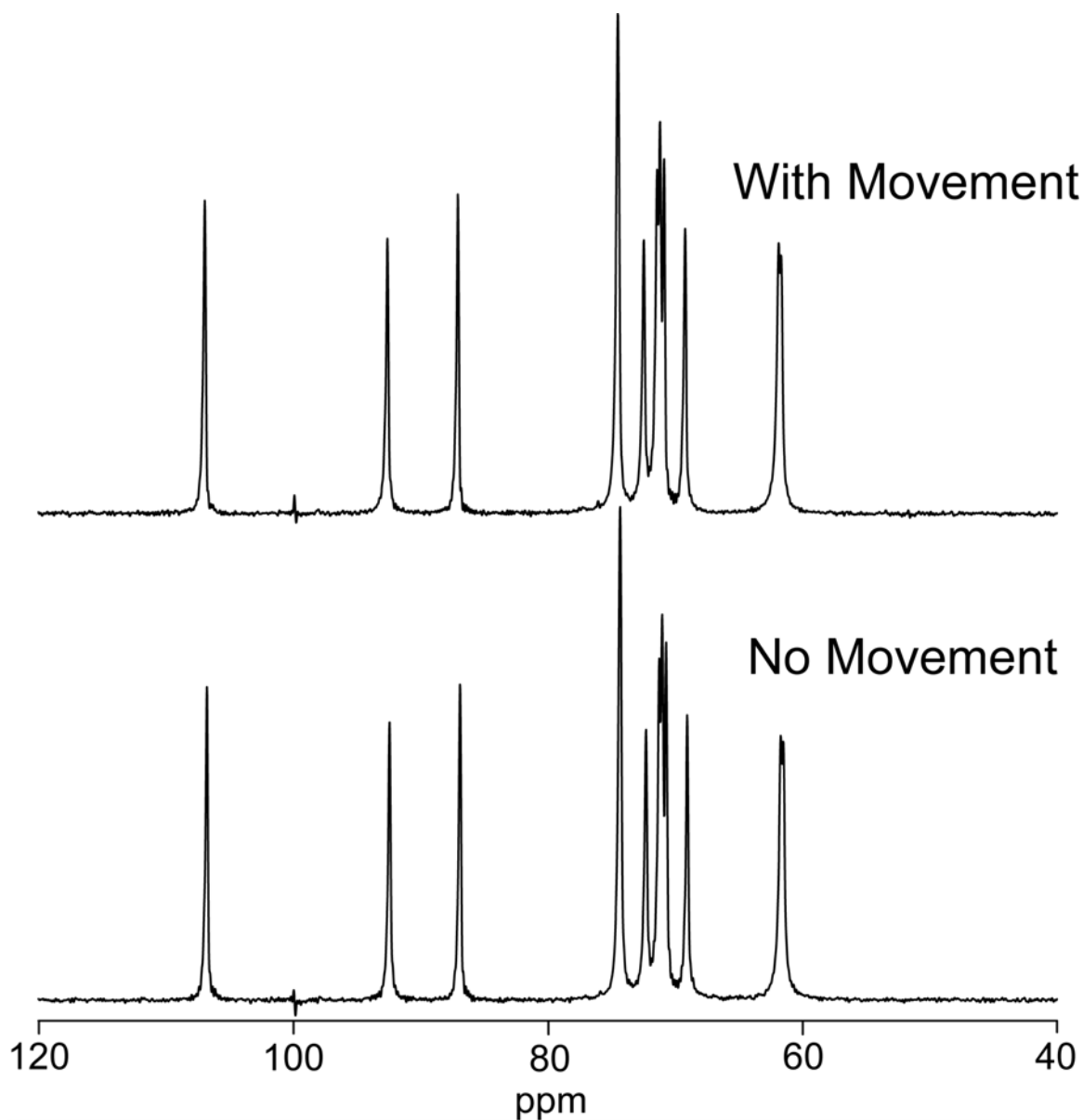


Figure 3.7. Individual spectra of MGA collected simultaneously in mss probe.

Slight differences in relative intensity of the acid peaks at 181.15 ppm are due to the accuracy of the magic angle setting. Due to mass differences of the individual samples, the SNR are also slightly different. These small differences aside, the spectra are identical, indicating that all four modules produce spectra of equal and high quality.



Two experiments with lactose monohydrate were performed to show the difference of relaxation to equilibrium in the homogeneous region of the magnet and at 17 cm from the homogeneous region. At 17 cm distance the field is ~95%. For the first experiment lactose was acquired with a 300 second pulse delay and was left in the homogenous region during acquisition and relaxation to equilibrium. In the second experiment a transient acquisition was done with the sample in the homogeneous region and then the linear actuator immediately moved the sample 17 cm from this sweet spot. Relaxation was allowed to occur at this distance for 299 seconds. At 1 second prior to acquisition the sample was moved back to the sweet spot and acquisition of the next transient performed. The results show no difference in spectral quality (Figure 3.8).



**Figure 3.8. Spectra of lactose monohydrate collected with and without probe movement.** The spectra show no difference in spectral quality with relaxation in (No Movement) and out of (With Movement) the homogeneous region of the static magnetic field.

### 3.4 Conclusions

The four-module mss probe can increase the throughput of a ssNMR spectrometer by up to four times with no compromise in spectral quality. Increased SNR per unit time for a sample can be done by running the same sample in all four modules. Besides the increase in length of the transmission lines to  $3\lambda/4$ , the mss probe utilizes proven probe

technology. The spinning modules can be located close enough together that the sample is never below an effective field of 95%. Tuning is accomplished outside of the magnet bore. Pharmaceutical solids, glasses, catalysts and polymers with longer  $T_1$ s are immediate applications for the mss probe. The advantage of the probe is increased at higher magnetic fields where  $T_1$ s are longer. Changes to the matching network in the receiver section of the spectrometer will eliminate the issues of the lossy high power solid-state RF switches.

### 3.5 References

1. Stejskal, E.O. and J.D. Memory, *High Resolution NMR in the Solid State*. 1994, New York: Oxford University Press. 189.
2. Metz, G., X.L. Wu, and S.O. Smith, *Ramped-Amplitude Cross Polarization in Magic-Angle-Spinning NMR*. J Magn Reson, 1994. **110**(2): p. 219-227.
3. Barich, D.H., et al., *3-Methylglutaric acid as a  $^{13}\text{C}$  solid-state NMR standard*. Solid State Nucl. Magn. Reson., 2006. **30**: p. 125-129.

## **Chapter 4**

### **Non Moving Multiple-Sample Solid-State NMR Probe**

## 4.1 Introduction

Multiple sample solid-state (mss) probes have been recently developed to take advantage of the long relaxation time of a sample to collect transient scans on other samples during this waiting period. Although the concept of interleaving experiments is sound and improves throughput, improvements are needed to address several major weaknesses in the first generation mss probes. The probes are long due to requiring three quarter wavelength ( $3\lambda/4$ ) coaxial transmission lines to accommodate the tuning segments of the RF circuits, which must be positioned outside of the magnet dewar for “remote” tuning. There is a need to have the superconducting magnet raised above standard height to accommodate the long probes and linear actuators. The linear actuator is necessary for moving the separate MAS modules into a single homogeneous region (“sweet spot”) of the  $B_0$  field for transient acquisition. Second, mechanical breakdown of the probes occurs due to the constant motion required to position each of the samples within the MAS modules sequentially into the “sweet spot” of the magnet. This motion of the probe can generate eddy current forces that may be detrimental to the superconducting solenoid.

Here, a new probe design has been developed that does not require a linear actuator to shuttle the modules into a single homogenous region, and also fits underneath standard height superconducting magnets. The non-moving multiple sample solid-state (nm-mss) probe contains two separate MAS modules that are in fixed locations within the two individual homogeneous regions of the static field. The signal from one sample in a MAS module can be acquired while the other sample is returning to equilibrium without the need for physically moving the samples. The performance of this new nm-mss probe

was tested to demonstrate comparability with existing single-sample probes and improvement over existing multi-sample probes.

## 4.2 Experimental

### 4.2.1 Probe concept

The basic probe design consists of two MAS systems that are located in the bore of the superconducting magnet. The design of this probe is shown in Figures 4.1 and 4.2.

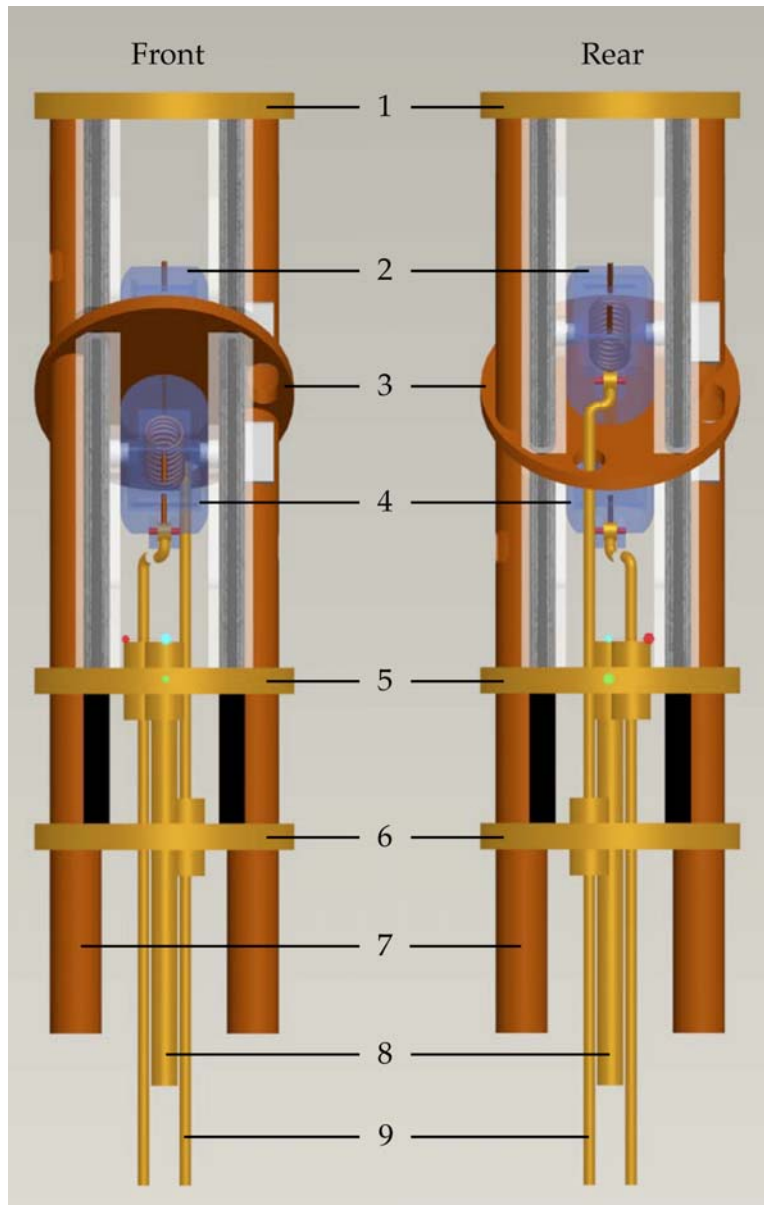


**Figure 4.1. Principle mechanical engineering assembly views of top section of the nm-mss probe.** 1) top plate; 2) top MAS module; 3) RF isolation plane; 4) bottom MAS module; 5) bottom plate; 6) plate to facilitate height adjustment; 7) transmission lines (Continued from bottom, Figure 4.2-1); 8) height adjustment screw; 9) magic angle adjustment rods.

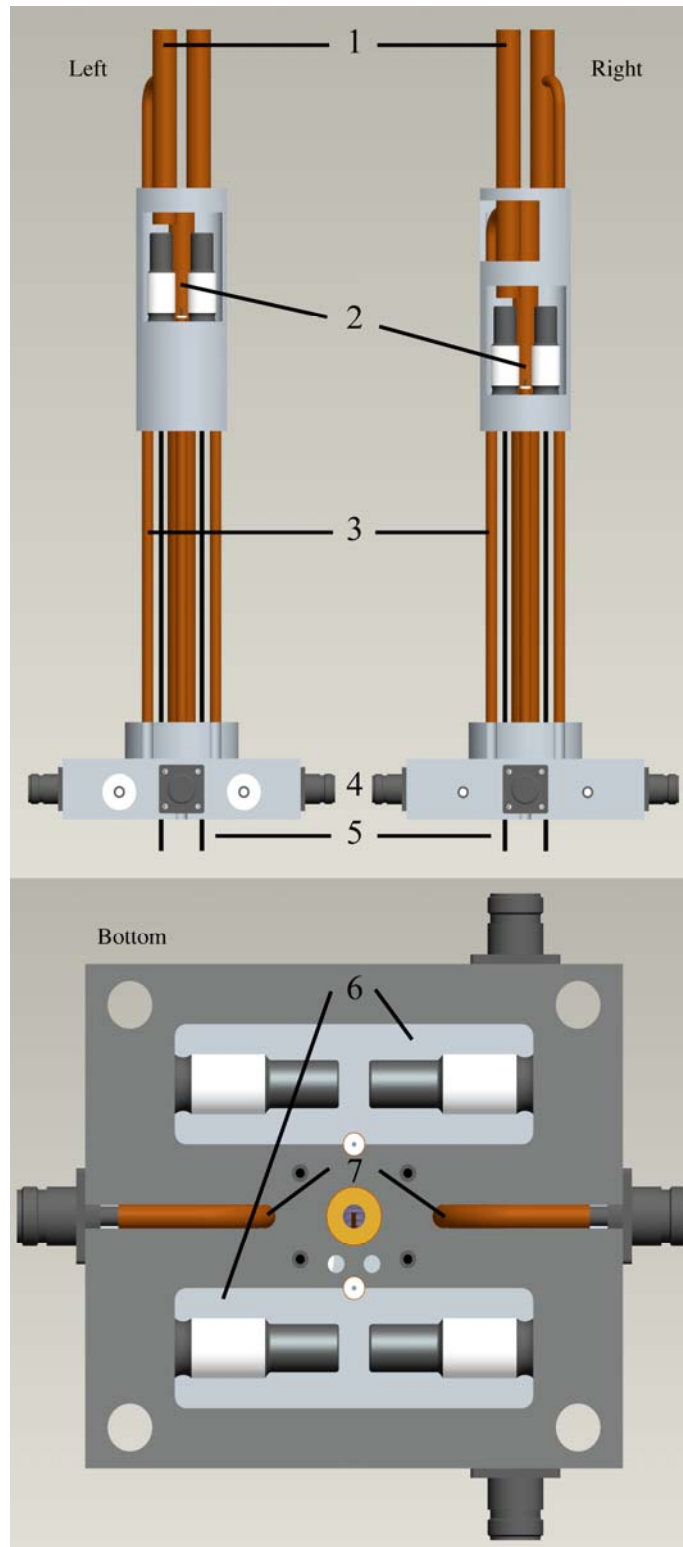


**Figure 4.2. Principle mechanical engineering assembly views of bottom section of nm-mss probe.** 1) Transmission lines (continue to top of probe, Figure 4.1-7); 2) Variable capacitors for proton tuning circuits (fixed capacitors not shown); 3) X RF to tap point; 4) RF power inputs; 5) Tuning wands; 6) Variable capacitors for X tuning circuits (fixed capacitors not shown); 7) RF to proton tuning circuits.



It has been found that there can be more than one relatively homogeneous region in the static magnetic field with a relatively inhomogeneous region between, and a depiction of this is shown in Figure 4.3. During testing of the mss probe relatively high resolution spectra were collected by switching between the modules without movement of the linear actuator. The MAS modules are each located in their own relatively homogeneous region of the magnet for signal acquisition. This eliminates the need for moving the probe with a linear actuator as previously reported. However, unlike the moving MSS probe, which can have any number of MAS modules limited only by space for the tuning elements,[1] this design is limited to two MAS modules.

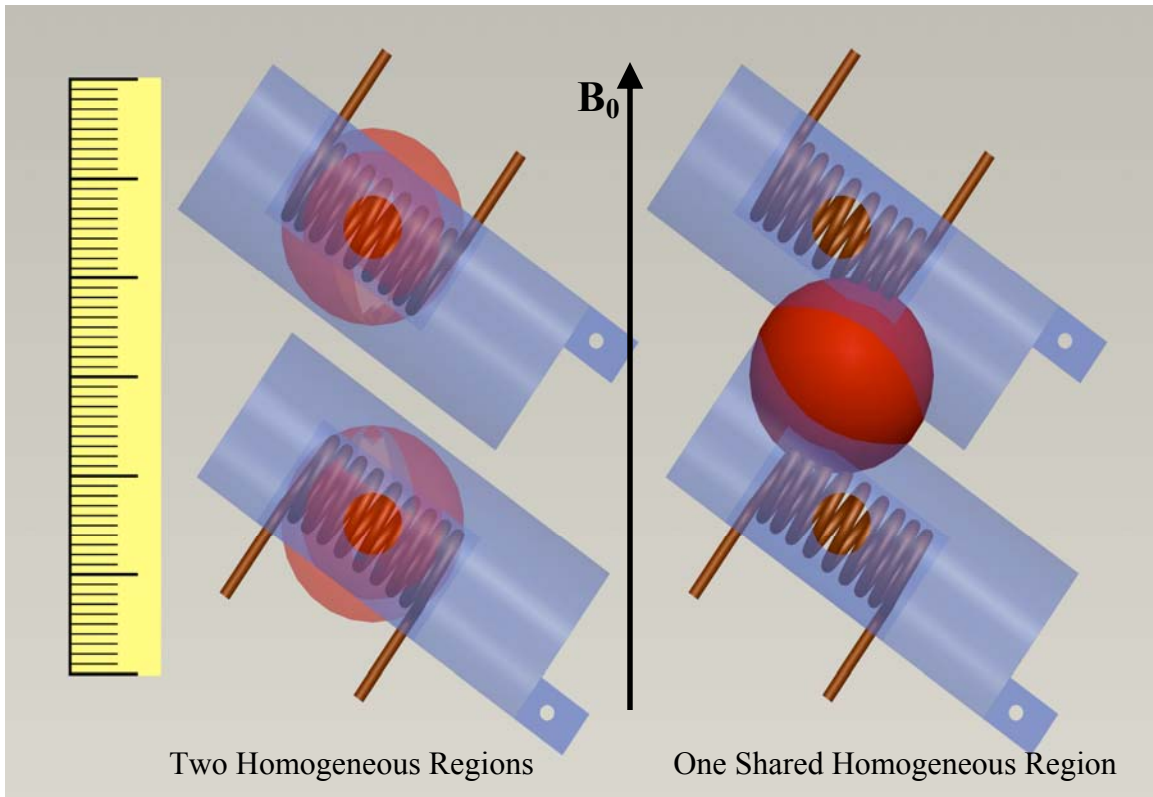


**Figure 4.3. Depiction of the modules in each of the two separate homogeneous regions, and sharing one homogeneous region.** A 6 cm ruler is added for perspective.  $B_0$  is the orientation of the static magnetic field.

While the sample is relaxing in one module, the other one can be pulsed. The pulse trains can be delivered using any desired pattern of switching because timing is not limited by mechanical translation of the sample. Therefore, the arrangement permits sequential analysis back and forth from module to module, or one module can be pulsed multiple times if the relaxation time for the sample in that module has a much shorter relaxation time than in the other module. The order in which the modules are to be pulsed is determined by the  $^1\text{H}$  T1s of the samples and done in a manner to acquire as many transients as possible in a given amount of time. Each spinning system features its own air supply lines for drive and bearing gas, RF connections, and magic-angle adjustment mechanism. Each module has independent spinning speed control, and may have variable-temperature capability and independent shimming parameters.

There are several advantages of this probe design. First, it has the capability of increasing throughput by a factor of two or more. More importantly, it would allow the analysis of samples that would not normally be run because of excessive use of spectrometer time, if the analysis time for one sample was several days. During that time, the samples in the other spinning module could be changed several times without disturbing the sample with the long analysis time. Moreover, this system has the capability of being automated so that the throughput advantage could be increased from 2 to 10 compared to a probe with no autosampler (i.e., if the samples were changed five times during an overnight run or over a weekend). If the choice is made to run the same sample in each MAS module the SNR per unit time would be increased by a factor of 1.4 by adding the two data sets together.

There should be little or no loss in field homogeneity, sensitivity, MAS speed, or  $^1\text{H}$  decoupling field strength compared to conventional NMR probes, nor is there a need to develop specialized spinning modules, pulse sequences, or RF technology. While this approach can be used at any magnetic field strength, it would be more advantageous at higher field strengths, where  $T_1$  relaxation rates are much longer than at lower field strengths.[2] Compared to previous MSS probes,[1] this probe will not suffer from potential mechanical breakdown due to constant probe motion and it also fits inside a standard shim stack.

This probe design is also very useful for studying nuclei in samples that have short relaxation times, such as many quadrupolar nuclei, because the probe movement does not limit the switching time between modules, as is the case with the previous mss probe designs.

There are also limitations to the probe design. For example, additional sample is needed if an increased SNR is desired, because two sample rotors would have to be filled instead of one. The modules are self-contained, which could limit the experiments to fixed angle, double resonance, and room temperature. Having two spinning modules/circuits will increase maintenance problems. Finally, having two spinning modules doubles the amount of compressed air needed to spin the samples. All of these limitations are relatively minor compared to the gains in throughput/sensitivity that would be achieved with this probe.

#### *4.2.2 Probe Construction*

Standard Revolution NMR (Fort Collins, CO) 7 mm spinning modules were used with slight modifications. The modules are 0.845" in diameter and spin 7 mm rotors up to 8000 Hz. Flexible plastic tubing (1/8" i.d.) supplies compressed air to Delrin® plastic supports. The Delrin® supports hold the spinning module in place and deliver the compressed air to the drive and bearing systems.

The receiver section of the  $^{13}\text{C}$  circuit, Figure 4.4, was modified in order to obtain better SNR results. Electro-mechanical 1P2T switches with TTL logic from Charter Engineering, Inc (Pinellas Park, FL) divert the high power RF pulses to the top and bottom modules. Pre-amplification of the signal is performed by low noise amplifiers from NuWaves Engineering (Middletown, OH) before it passes through a Miteq, Inc. (Hauppauge, NY) switch to return to the spectrometer receiver. With this design each MAS module/circuit can be selected independently for tuning and signal acquisition. Second, it allows the signal from the coil to go through a pre-amp before going through a switch, which yields a vast SNR improvement compared to having the signal go through a high power switch before the pre-amp.

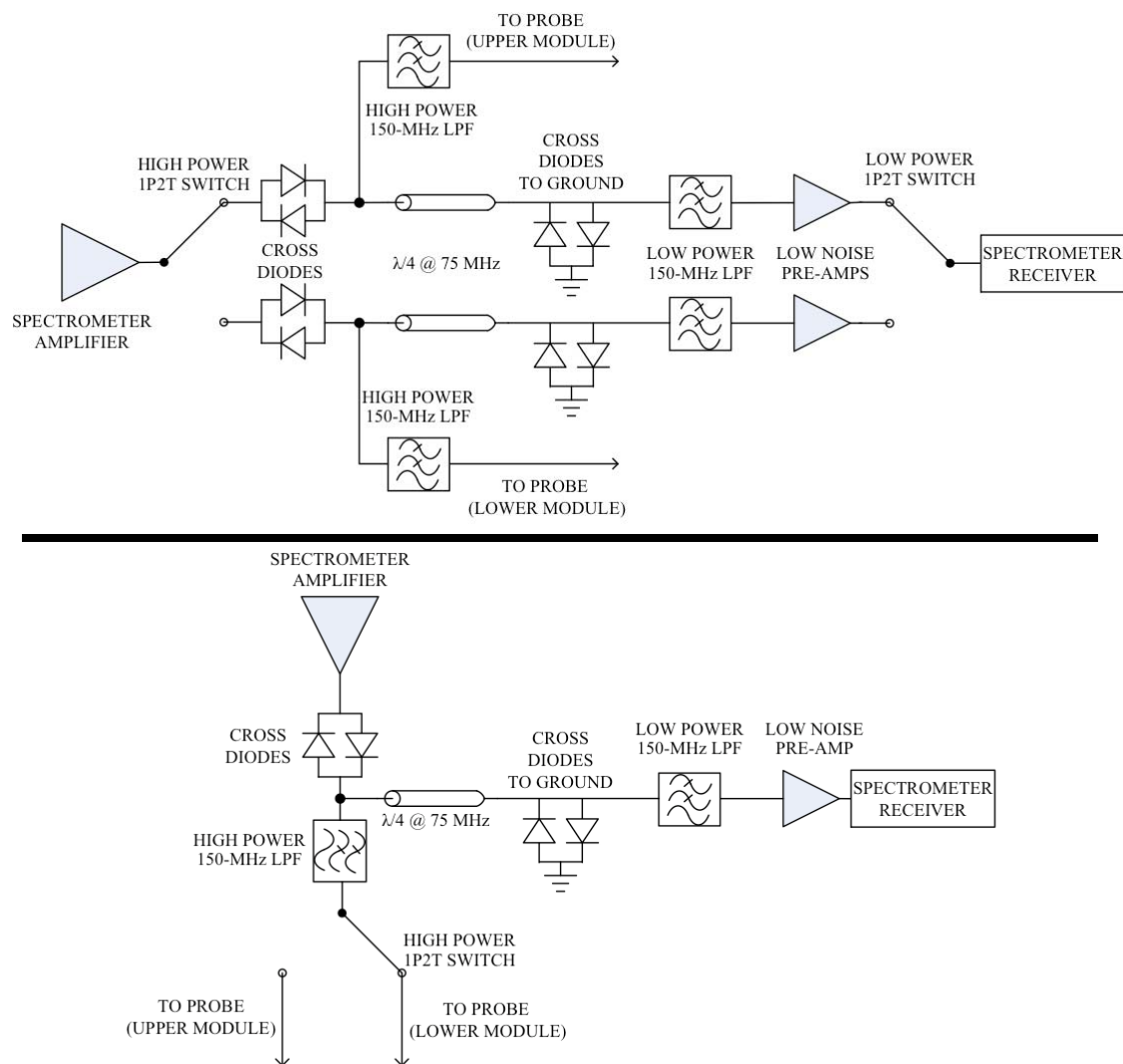


**Figure 4.4. Block diagrams of  $^{13}\text{C}$  receiver sections.** The top circuit configuration produces superior SNR, while the bottom circuit configuration minimizes the number of elements.

American Technical Ceramics (Huntington Station, NY) fixed capacitors and Polyflon variable capacitors (Norwalk, CT) are used to tune and impedance match the circuit. The position and arrangement of the capacitors in the tuning circuits are shown in Figure 4.2. A transmission line with quarter wavelength ( $\lambda/4$ ) isolation tap point was made by using 1/2" copper tubing for the outer conductor and 3/16" solid copper wire for the center conductor with Teflon grommets for support. These transmission lines transfer the RF from the tuning elements to the coil. Tuning wands made of mixed plastic and

brass parts are used to adjust the variable capacitors from outside the magnet. 1/4" semi-rigid copper coaxial cable supplies RF power to the  $^1\text{H}$  tuning circuit and transmits RF power from the  $^{13}\text{C}$  tuning circuit to the  $\lambda/4$  tap point. The coil is made from 11 turns of 16 gauge solid copper wire. This coil configuration maximizes the number of turns over the allowed length for the coil in the MAS module.

The samples in the MAS modules were located less than 3 cm apart in the probe. The lower module can be raised or lowered independently from the top module while actively pulsing the probe. Movement of the lower module is coupled to movement of its magic angle adjustment mechanism in order to minimize the magic angle deviation during movement. An aluminum cylinder with 0.05 inch wall thickness encloses everything from the  $^1\text{H}$  tuning circuits to the top of the probe.

#### *4.2.3 Solid-State NMR Spectra*

All spectra were acquired using a Tecmag (Houston, TX) Apollo SSNMR spectrometer equipped with a Oxford (Oxford, UK) 89 mm bore superconducting magnet operating at 75.9 MHz for  $^{13}\text{C}$ . Samples were spun at the magic angle at rates ranging from 3 to 4 kHz, and were independently controlled via spin speed controllers from Revolution NMR, LLC (Fort Collins, CO). Ramped cross polarization[3] was used to acquire all spectra. Proton decoupling powers of 40-80 kHz were used to acquire all spectra.

Acquisition parameters for hexamethylbenzene (HMB) were: 512 data points, 17 ms acquisition time, and the data were zero-filled to 4096 points prior to Fourier transform (FT). Acquisition parameters for 3-Methylglutaric Acid (MGA) were: 3072

data points, 103 ms acquisition time, and the data were zero filled to 32,768 points prior to FT. Acquisition parameters for Adamantane were: 5120 acquisition points, 172 ms acquisition time and the data were zero filled to 65,536 points prior to FT. All spectra were collected with a 30 kHz spectral width. No apodization was used. Signal to noise ratio (SNR) measurements of 12 transient scans of HMB and MGA spectra were made by using a noise window sampled over a 30 ppm chemical shift range, and signal intensity was determined from the methyl peak of each (17.35 ppm for HMB and 18.84 ppm for MGA). Determination of MAS module position in a homogeneous region of the superconducting magnet was performed using adamantane line widths. The setting of the magic angle was facilitated by monitoring the acid peaks of MGA, which have baseline resolution when the proper angle is reached.[4]

### **4.3 Results**

#### *4.3.1 Homogeneity and Signal to Noise Ratio*

Adamantane was loaded into the top MAS module and the probe position was adjusted until satisfactorily narrow lines were observed. After locking the main body of the probe height and rotation relative to the magnet dewar, the adamantane sample was transferred to the bottom MAS module. The height of the lower module was adjusted until satisfactorily narrow adamantane lines were observed. As seen in the spectra in Figures 4.5 and 4.6, it is possible to have both modules in separate homogeneous regions that produce adamantane line widths of less than 7 Hz. It must be noted here that no shim stack was used for these experiments, and line widths of less than 7 Hz is quite good when only sample positioning is used for optimization. The top module yielded a line width of 6 Hz and the lower module 6.4 Hz. These line widths are satisfactory for

pharmaceutical samples and the 0.4 Hz difference should not be of consequence in obtaining quality data, and again the difference could be nullified with the use of a shim stack. If the bottom module is moved even closer to the top module the homogeneity would decrease and the line width for adamantane broadens (data not shown). This is because of the effect depicted in Figure 4.3-A, where there is a less homogeneous region of space between the two relatively homogeneous regions in which the samples are located.

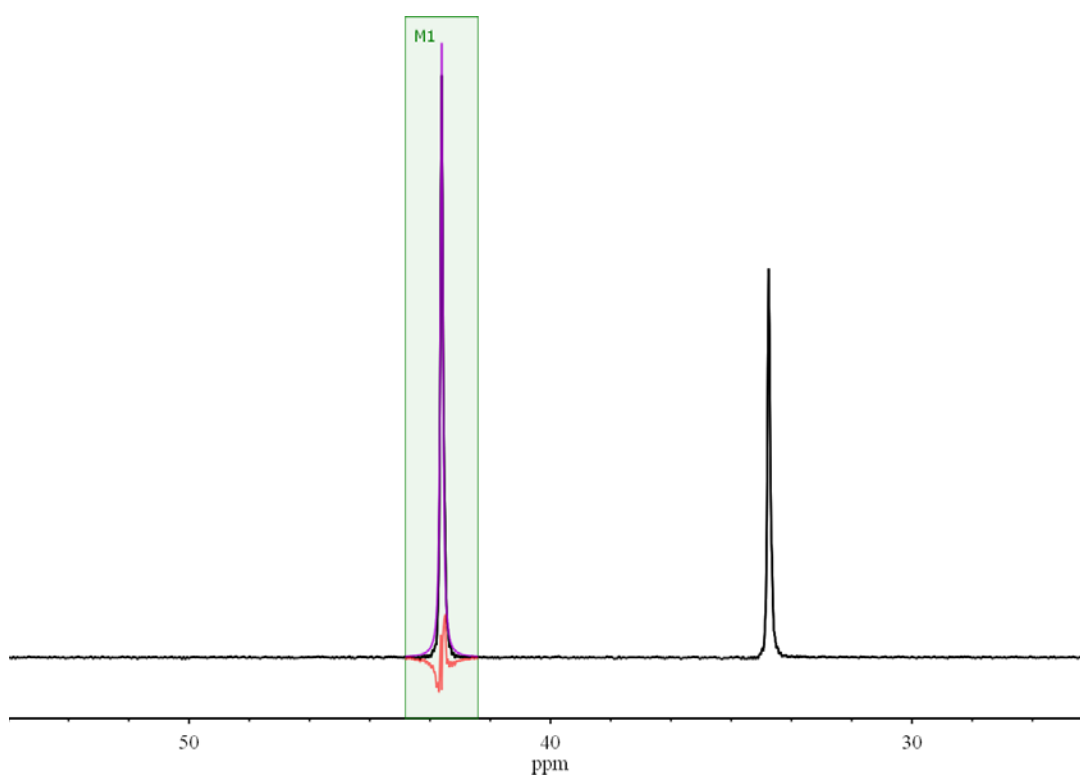


**Figure 4.5.**  $^{13}\text{C}$  Spectrum of adamantane obtained from the top MAS module of the nm-mss probe has a line width of 6 Hz.



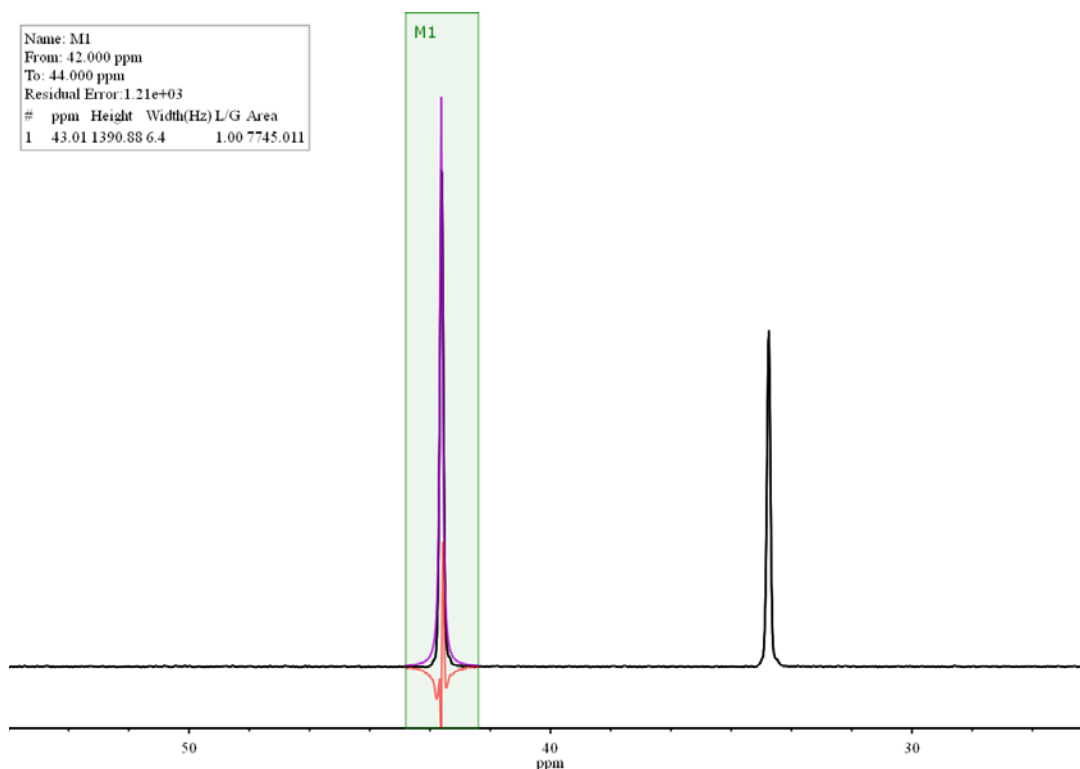


**Figure 4.6.**  $^{13}\text{C}$  Spectrum of adamantane obtained from the bottom MAS module of the nm-mss probe has a line width of 6.4 Hz.

SNR measurements were made with both HMB and MGA. A comparison of the SNR for the nm-mss probe to conventional probe technology is shown in Figures 4.7 and 4.8. The spectra for the comparison experiments were done with the high power RF switches in place for both the nm-mss and conventional probe. The HMB SNR for the top module of the nm-mss probe was 408 (similar for the bottom module, but not shown) and 361 for the conventional probe. MGA SNR measurements were also made for comparison and were 158 for the nm-mss probe and 168 for the conventional probe. SNR was reproducible within 5% on consecutive acquisitions. However, there is a significant difference in the power handling between the two probe technologies. In order to obtain a  $^1\text{H}$   $90^\circ$  pulse width of  $3.0\ \mu\text{s}$  ~30% more power was required. This is not surprising. The transmission line in the conventional probe is four times larger than those in the nm-mss probe. Also, the ratio of inner conductor to outer conductor of the

nm-mss probe transmission lines may not be ideal due to limited available size combinations from vendors.

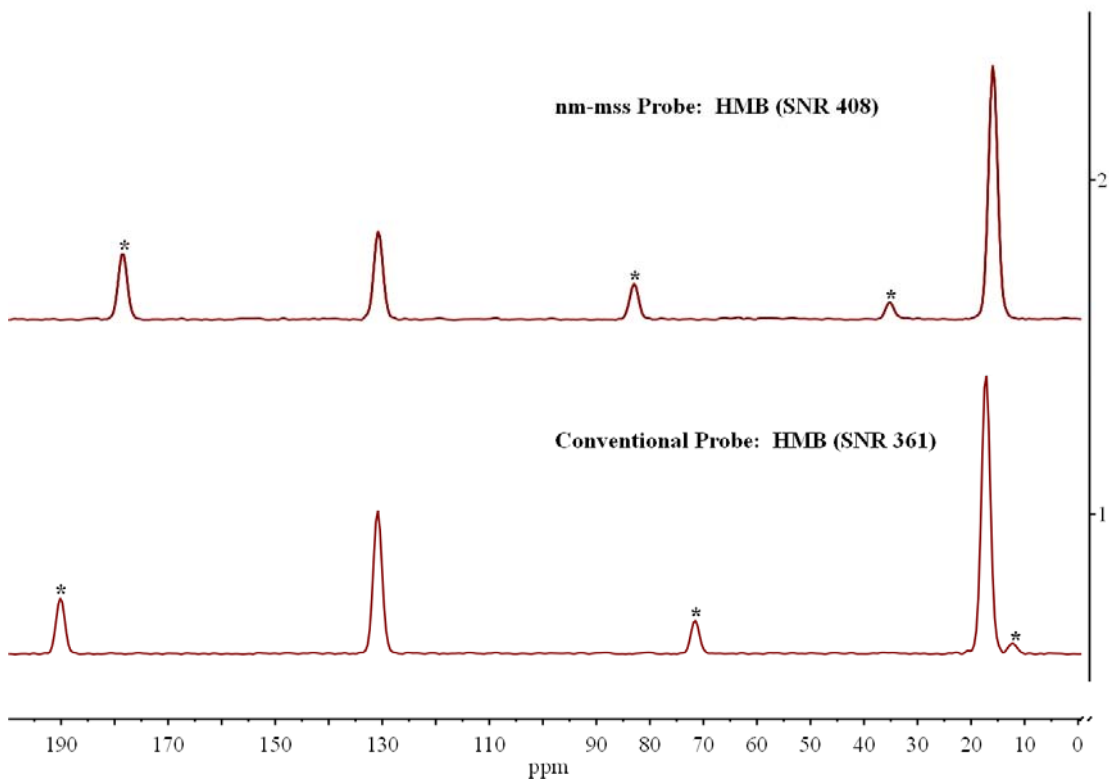


**Figure 4.7.**  $^{13}\text{C}$  spectra of HMB from nm-mss probe and a conventional probe (\* denote spinning sidebands). SNR Measurements use the methyl peak at 17.35 ppm.

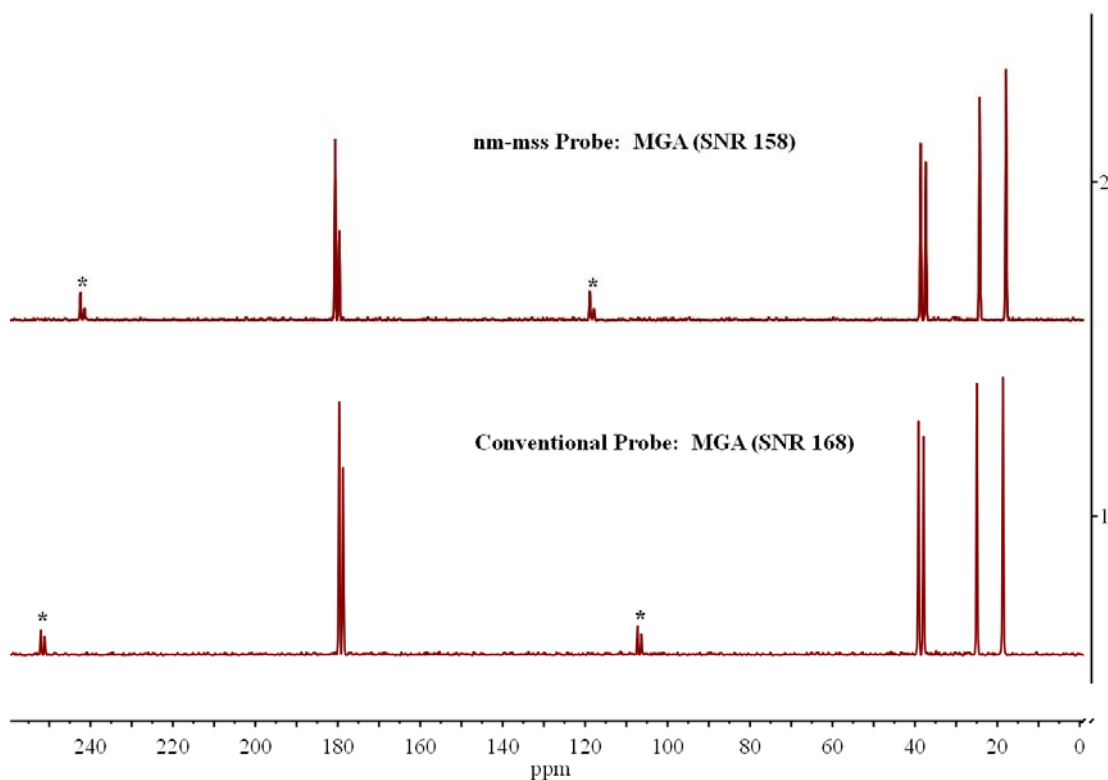


**Figure 4.8.**  $^{13}\text{C}$  spectra of MGA from nm-mss probe and a conventional probe (\* denote spinning sidebands). SNR measurements use the methyl peak at 18.84 ppm.

The receiver section of the  $^{13}\text{C}$  circuit had to be modified due to loss of signal when it had to pass through the high power RF switch, as discussed in Chapter 3. Once the change was made to the superior circuit shown in Figure 4.4 a 20% improvement in SNR resulted and representative spectra are shown in Figure 4.9. The new circuit does require two of many components, but the increase in cost for the second module is very inexpensive compared to the time savings of increased SNR.

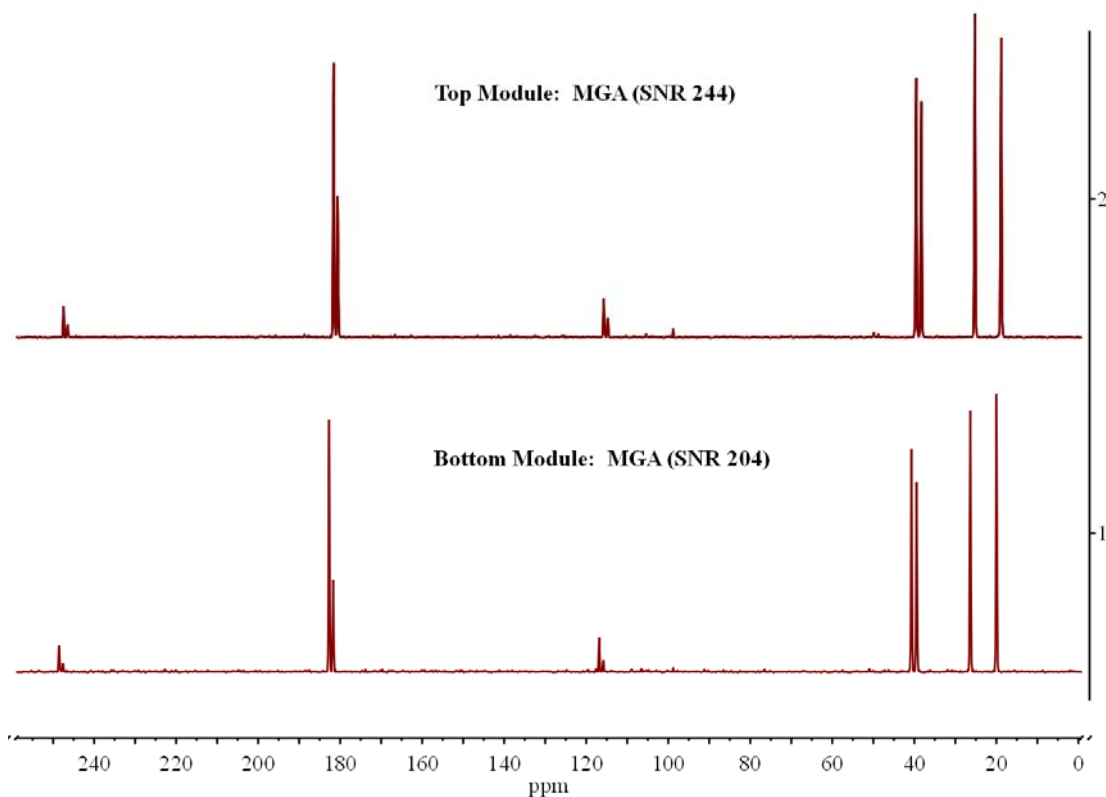


Figure 4.9.  $^{13}\text{C}$  spectra of MGA acquired simultaneously using a superior  $^{13}\text{C}$  receiver section.

#### 4.3.2 RF Isolation

Two MAS modules in such close proximity causes concern over possible crosstalk and coil coupling. Crosstalk will be defined here as the signal appearance from one sample in the spectrum of the other. Coil coupling is when  $^1\text{H}$  RF pulses on one sample cause the protons spins in the other sample to not properly relax to equilibrium with the static magnetic field.

To investigate the signal crosstalk possibility an experiment with adamantane and HMB was devised. Adamantane was selected because it has a very large amount of signal (SNR of up to 1000 in 4 scans). HMB was selected to save time based on its relatively short  $^1\text{H}$   $T_1$  and lack of peaks that overlap those of adamantane. 5000 transient scans of HMB were acquired normally while adamantane was spinning in the adjacent

MAS module. Absence of signal crosstalk is apparent in Figure 4.10. This result is as expected. In order to observe signal crosstalk two things must happen. First, the RF pulses must be strong enough to cause sufficient proton spin vector angle from  $B_0$  followed by sufficient cross polarization RF pulses to transfer the magnetization from the protons spins to the  $^{13}\text{C}$  spins. Second, in the unlikely event that there is signal generated from the sample not located inside the coil that was directly pulsed, a very weak signal must be detected from centimeters away.

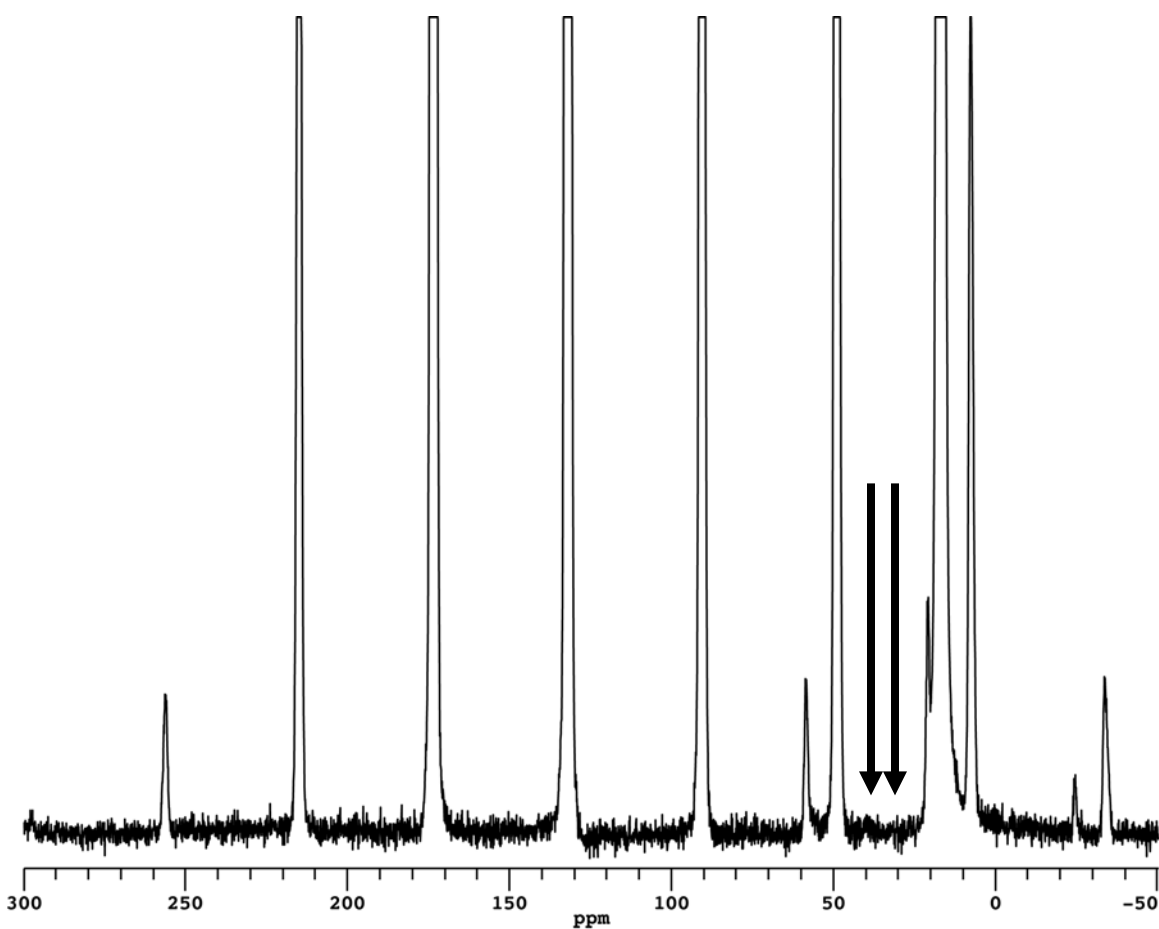


**Figure 4.10. Expansion of the noise region of 5000 transient scans of HMB.** Peaks for adamantane would be at 40 and 31.5 ppm as indicated by the arrows, but none are present.

Investigation of  $^1\text{H}$  RF pulses causing changes in  $^1\text{H}$  spin lattice relaxation back to equilibrium requires a chemical with a relatively long  $^1\text{H}$   $T_1$  and one with a relatively

short  $^1\text{H}$   $T_1$ . Xylose ( $T_1 \sim 200$  s) and MGA ( $T_1 \sim 1$  s) were used to satisfy these parameters. For the experiment the module containing MGA was pulsed 1, 15, and 60 times followed by a single pulse on the xylose containing module. In the case where MGA was pulsed once, the sequence was: pulse MGA; 300 s pulse delay (PD); pulse xylose. The sequence for the 15 and 60 MGA pulses prior to a xylose pulse had pulse delays of 20 s and 5 s respectively. The net result of the pulse sequences in all three versions of the experiment is the xylose was pulsed every 300 s. If relaxation of the xylose was affected by the pulses on MGA, the signal intensity of the peaks in the xylose spectrum would be expected to decrease. Table 4.1 contains the peak intensity for xylose in the three experiments with MGA and that of xylose collected alone.

**Table 4.1. Xylose peak intensities for experiments in coil coupling.**

Experiment	Peak Intensity at 72.26 ppm (arbitrary units)
60 MGA Pulses	5278
15 MGA Pulses	8731
1 MGA Pulse	8441
Xylose Alone	8337

The data for xylose alone is normalized to the parameters of the other 3 experiments, because the spectrum used had been previously collected with 32 scans and a 480 s pulse delay. Normalization to 4 scans was performed by dividing the peak intensity of 32 scans

by 8. The Bloch equation:  $M_z = M_{z_0} \left( 1 - e^{\left( \frac{-x}{T_1} \right)} \right)$  where  $M_z$  is the signal intensity with a

PD of  $x$  seconds, and  $M_{z_0}$  is the intrinsic signal intensity (100% relaxation to equilibrium). The data suggests that there is perturbation to relaxation of xylose caused by the pulses on MGA. The cumulative perturbations are not of sufficient magnitude to be measurable for the 1 and 15 preceding MGA pulses, but it is sufficient to be

measurable in the case of 60 preceding MGA pulses. This is considered to be a positive result as the situation of pulsing 60 times more on one sample will probably be rare. We expect that more similar samples will be run at the same time in the probe for comparison to each other, i.e. two formulations of a particular API. The xylose spectra are shown in Figure 4.11.

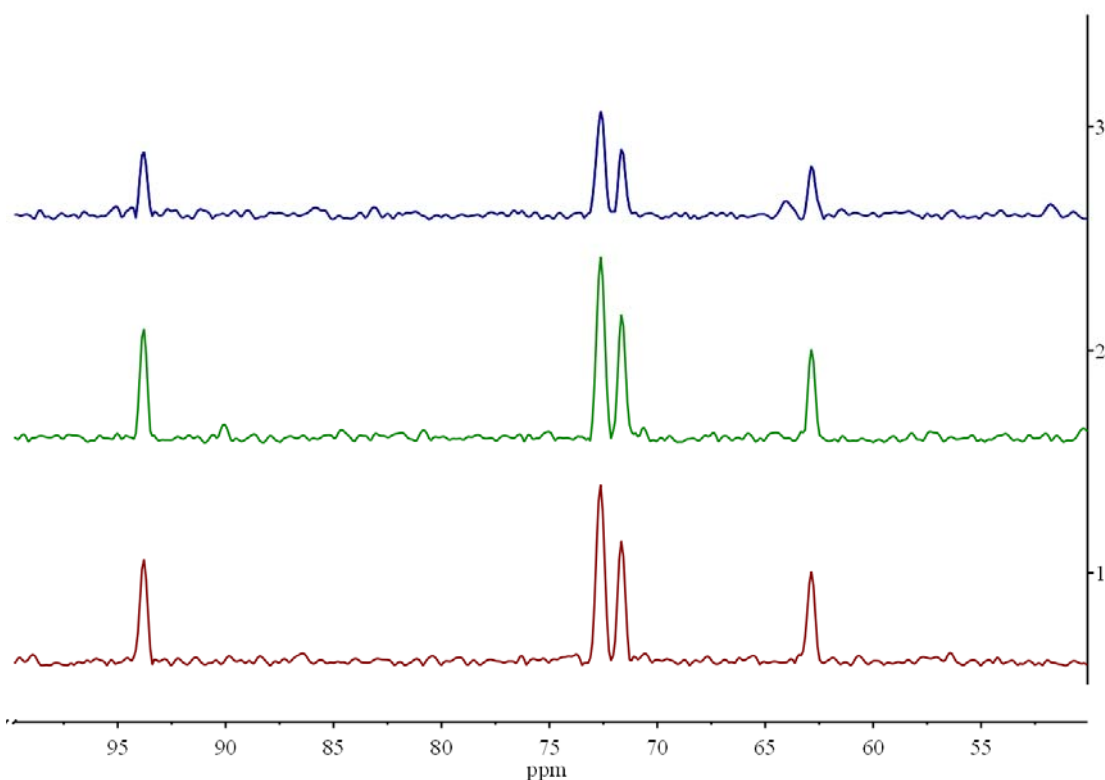


**Figure 4.11.**  $^{13}\text{C}$  spectra of xylose with MGA pulses prior to acquisition. 1) 1 MGA pulse; 2) 15 MGA pulses; 3) 60 MGA pulses

We also determined that the cable length between the high power RF switch and the probe can have an effect on the  $^1\text{H}$  RF isolation. A small receive coil was fashioned to fit inside of a MAS rotor. This rotor and receive coil was then placed inside the sample coil of the bottom MAS module to measure the amount of radiation experienced by a sample. The peak to peak voltage of the receive coil was measured with an

oscilloscope. When the bottom sample coil, which directly contains the receive coil, was pulsed, 2.74 V was measured. A pulse on the top sample coil produced 8.85 mV on the receive coil when no cable was connected to the containing module's  $^1\text{H}$  RF circuit. A 153 cm cable was next connected to the containing module  $^1\text{H}$  RF circuit with the distal end of the cable open circuited, as it would be when unselected by the high power RF switch. The length of the cable was incrementally shortened and the receive coil voltage was measured at each increment. A graph of these measurements is shown in Figure 4.12.

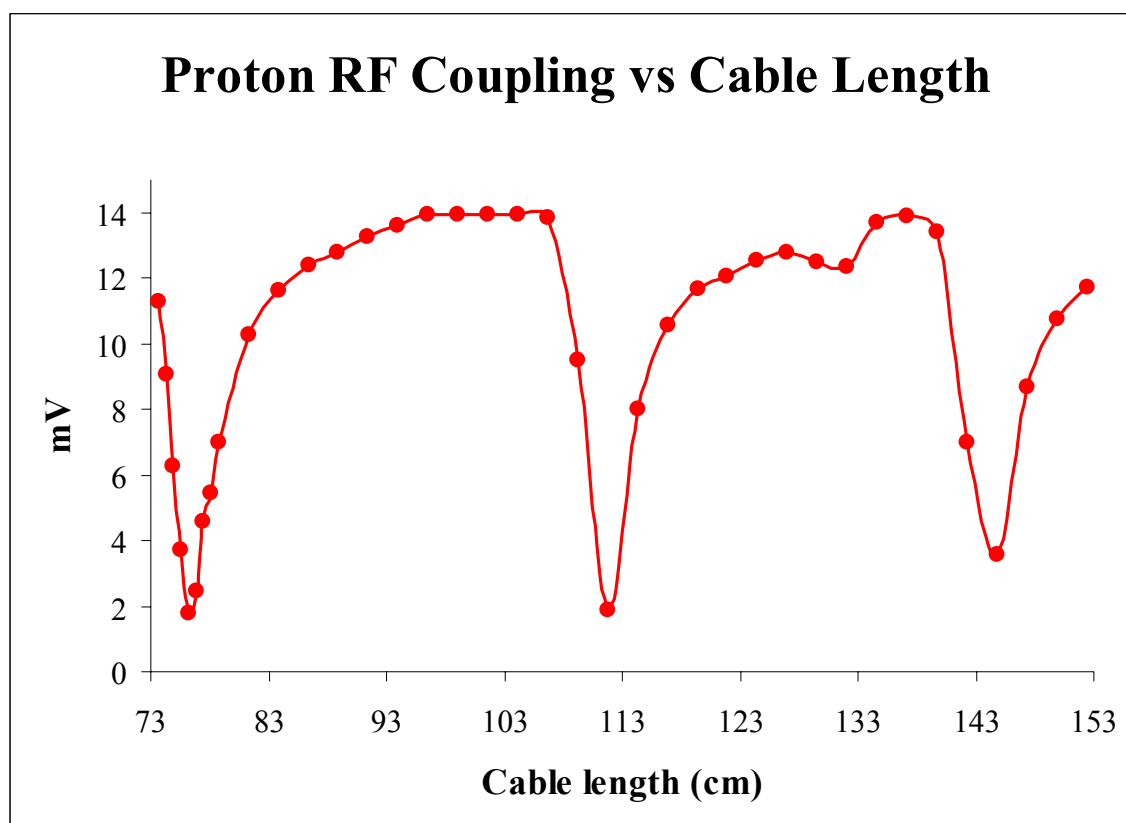
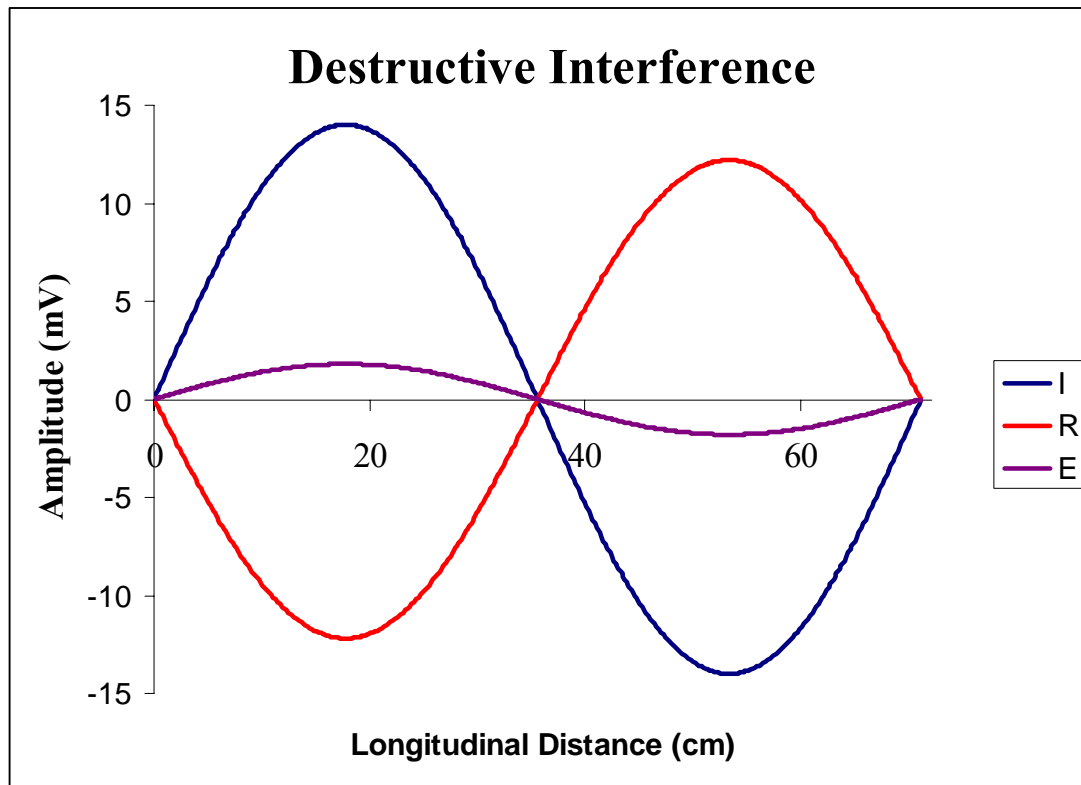


Figure 4.12. Graph of  $^1\text{H}$  RF coupling of sample coils vs. attached open circuited cable length



The minima are evenly spaced at 33 cm intervals. This interval is equal to the half wavelength ( $\lambda/2$ ) at a frequency of 300 MHz in a cable with a velocity of propagation equal to 0.7 c, which is standard for Teflon dielectric coaxial cable.

The two-way propagation of the initial received signal on the sample coil results in a 180 degree phase change, which upon retransmitting somewhat destructively interferes with the signal received on the receive coil. The signal cancellation on the receive coil is not completely destructive as the reflected and retransmitted signal is attenuated by the cable. A graphical depiction of destructive interference is shown in Figure 4.13. The result is an improvement of 20 dB isolation by simply choosing the proper cable length, which in this case is 145 cm.



**Figure 4.13. Graphical depiction of theoretical deconstructive interference caused by circuit path length equal to an odd multiple of the quarter-wavelength. I) Incidental signal; R) Reflected and retransmitted signal; E) Effective received signal.**

#### 4.4 Conclusions

The nm-mss probe has been shown to work tremendously well for a first generation prototype. Both modules can be located in their own relatively homogeneous region of the static magnetic field. The SNR is comparable to conventional probe technology. There are higher RF power requirements for  $^1\text{H}$  90 pulses, but this is to be expected based on the size and composition of the transmission lines. The additional power requirement is still below 500 watts, which introduces no problems for the probe. The results show that the isolation between the modules is satisfactory to a reasonable extent to realize the time saving element of its use in practice. When 60 pulses on the other module precede the acquisition of xylose there was a uniform loss of approximately 30% signal intensity, but this is a very extreme case. Also, the cable length for the MGA/xylose experiments was 153 cm, which has been shown to be suboptimal. With a proper cable length RF isolation is optimized.

#### 4.5 References

1. Nelson, B.N., et al., *Multiple-sample probe for solid-state NMR studies of pharmaceuticals*. Solid State Nucl. Magn. Reson., 2006. **29**: p. 204-213.
2. Harris, R.K., *Nuclear Magnetic Resonance A Physicochemical View*. 1989, New York: John Wiley and Sons, Inc. 260.
3. Metz, G., X.L. Wu, and S.O. Smith, *Ramped-Amplitude Cross Polarization in Magic-Angle-Spinning NMR*. J Magn Reson, 1994. **110**(2): p. 219-227.
4. Barich, D.H., et al., *3-Methylglutaric acid as a  $^{13}\text{C}$  solid-state NMR standard*. Solid State Nucl. Magn. Reson., 2006. **30**: p. 125-129.